# Resonant phonon-based THz quantum-cascade lasers and real-time T-rays imaging

*Qing Hu* (MIT)

**IQCLSW Workshop, Monte Verita, Switzerland**
**September 15, 2008**

Promising applications at THz frequencies, and THz "gap" for semiconductor sources.

- THz quantum-cascade lasers with:
  - resonant-phonon depopulated THz gain medium,
  - metal-metal waveguides for THz mode confinement.
- Real-time THz imaging using focal-plane array camera.

# Several Important Applications at THz frequencies

## See through opaque materials with spectral fingerprints

- Terahertz (1-10 THz, $\lambda \approx$ 30-300 $\mu$m, or $\hbar\omega \approx$ 4-40 meV) range corresponds to rotational/vibrational energy levels in molecules, which tend to have a large radiative dipole moment (*eg.* OH at 2.510 THz and 2.514 THz, monitored by NASA MLS/EOS).
- Chemical gas sensing, agent detection.
- T-rays imaging for medical applications. Cancerous cells have higher water and blood concentrations, different absorption from normal cells.
- Explosives and drug detection in security and drug enforcement applications.
- Biosensing, stretching and twisting modes in DNA. These low-frequency modes are associated with specific species.
- Plasma diagnostics in fusion experiments.
- In long term, high-bandwidth wireless communications, and high-speed signal processing.

# Terahertz "fingerprints" of several explosives

**(in semi-log plots)** Source: X.-C. Zhang (4/2007)

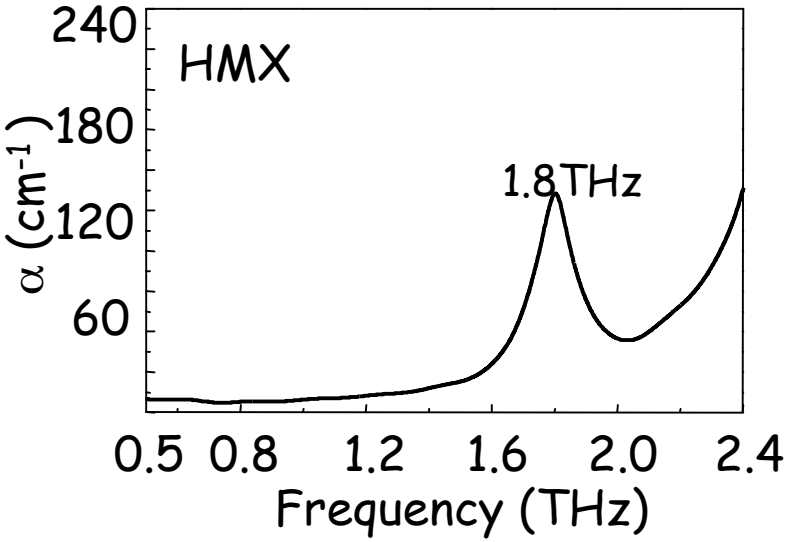


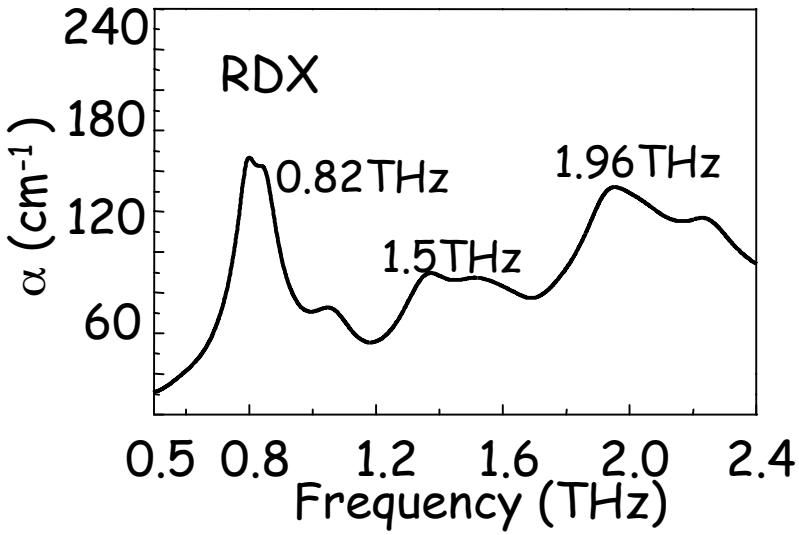


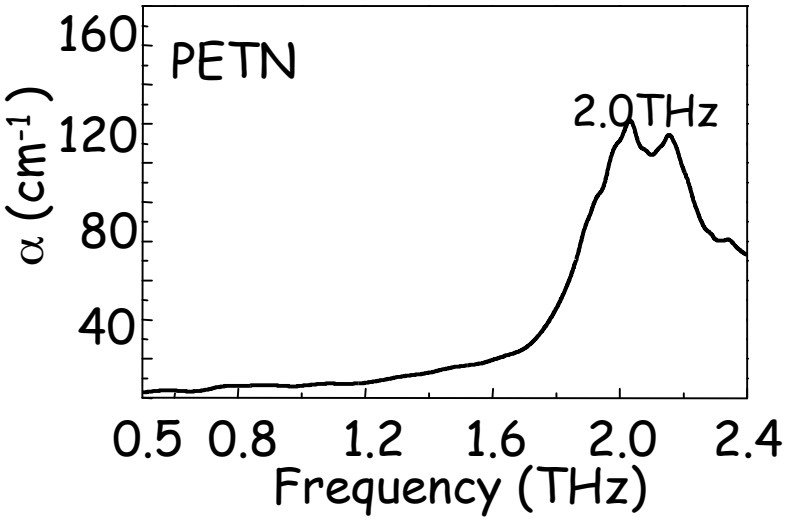


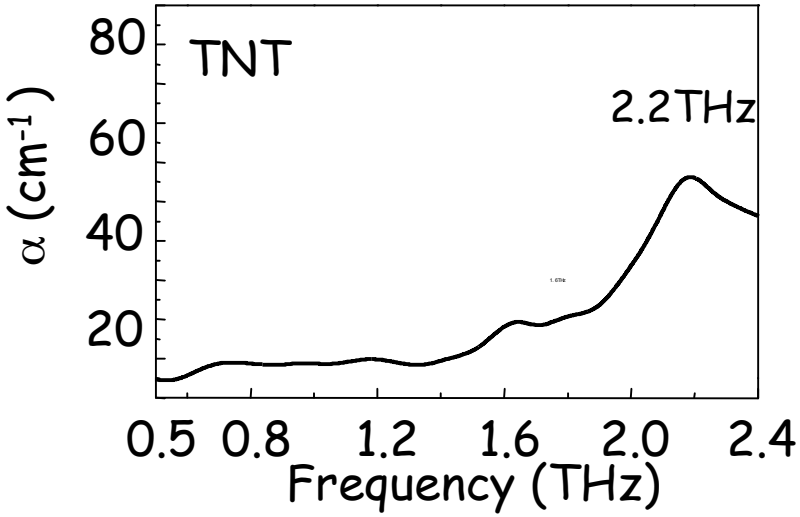

# TNT “phonon” mode at 3.48-THz (116 $cm^{-1}$)

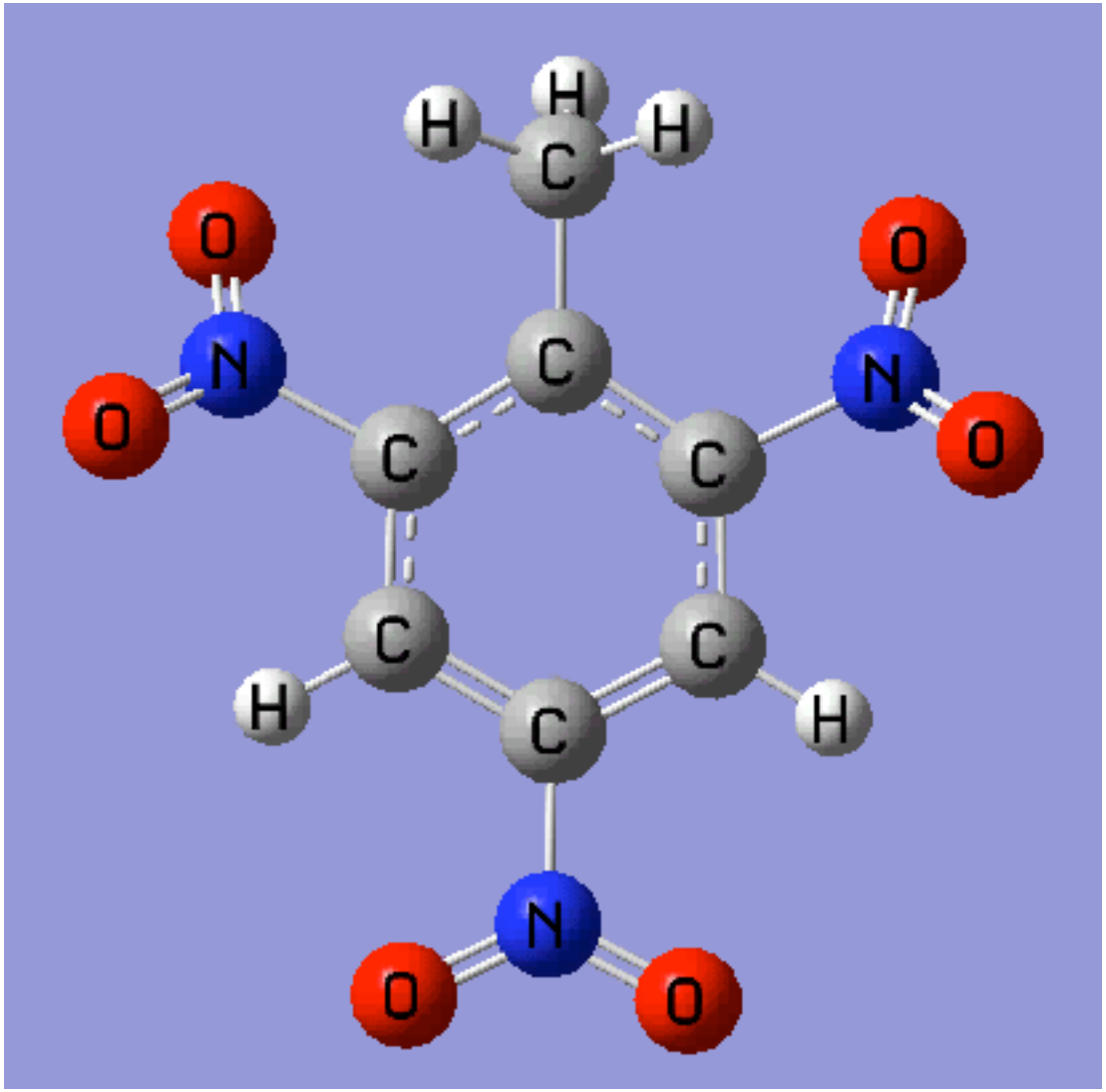


Courtesy X. C. Zhang at RPI.

# T-rays imaging for drug detection

(K. Kawase, OPN, October 2004)

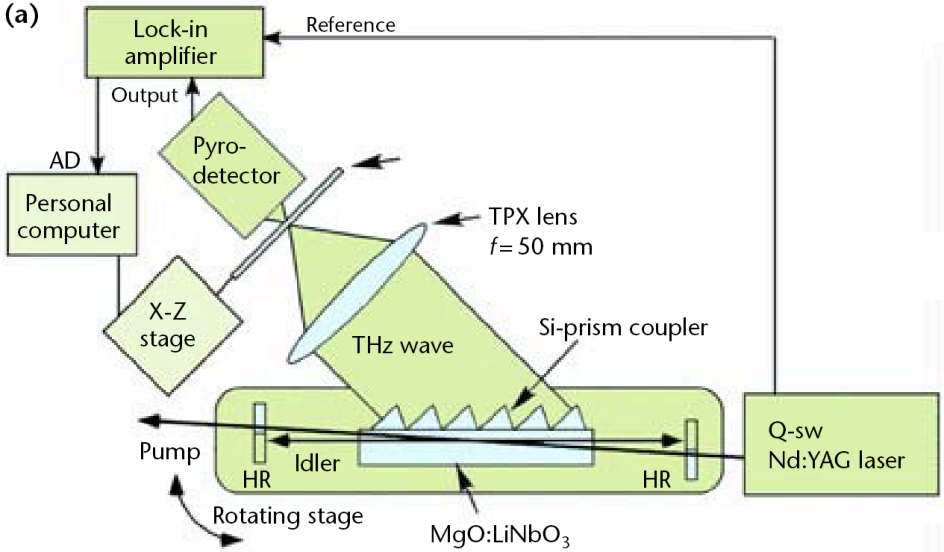


Three different drugs, MDMA (left), aspirin (center), and methamphetamine (right), have different images in T-rays.

Pictures taken with a THz OPO (1.3-2 THz) and mechanical scans.


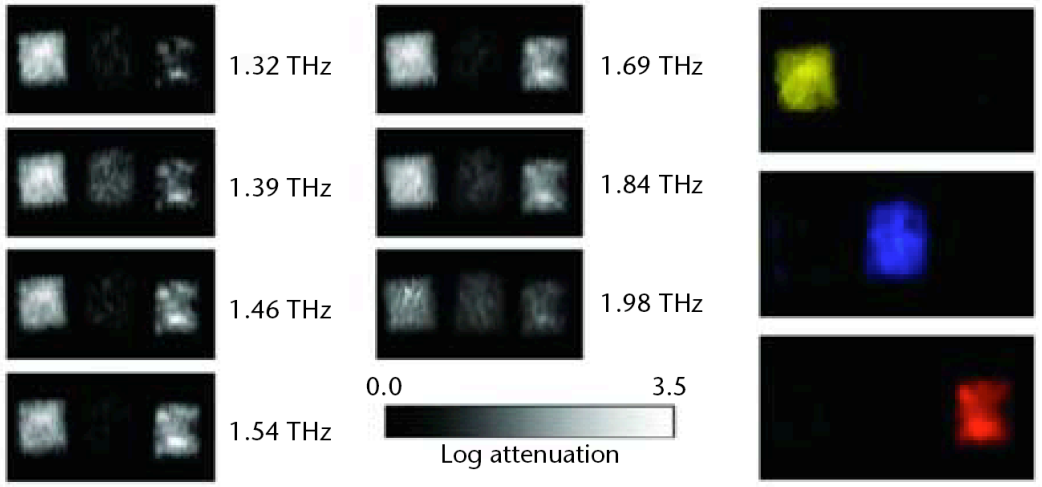

# Desired T-rays imaging systems

- Sources:
  - Compact and solid-state with >10 mW output;
  - easy to operate, above liquid nitrogen temperature in the near term, above TE cooler and even room temperature eventually;
  - multicolor, covering a broad frequency range (1-10 THz);
  - frequency tunable;
  - phase-locked with narrow linewidth (for sharp spectral fingerprint detection).

- Detectors:
  - Focal-plane arrays at video rate (>10 frames/sec.) for real-time imaging and screening.

# However, "THz gap" is in the way to fully utilize this E&M spectrum

- THz gap, what is it and what is its origin?
- There is no THz gap in passive components, *i.e.* mirrors, waveguides, filters, polarizers, focusing elements. They tend to be more difficult (or easier) to fabricate as the frequency gets higher.
- For active devices, there is no THz gap in detector technology. Bolometric detectors, both direct and heterodyne, cover a broad frequency range that is determined by the energy absorber. For photodetectors, SIS works at ≤1.5 THz, impurity FIR detectors at >1.5 THz, and interband HgCdTe at >15 THz.
- There is only THz gap in sources, more specifically, solid-state sources based on semiconductor materials.

# Power Performance of Solid-State Sources
## — the existence of THz gap

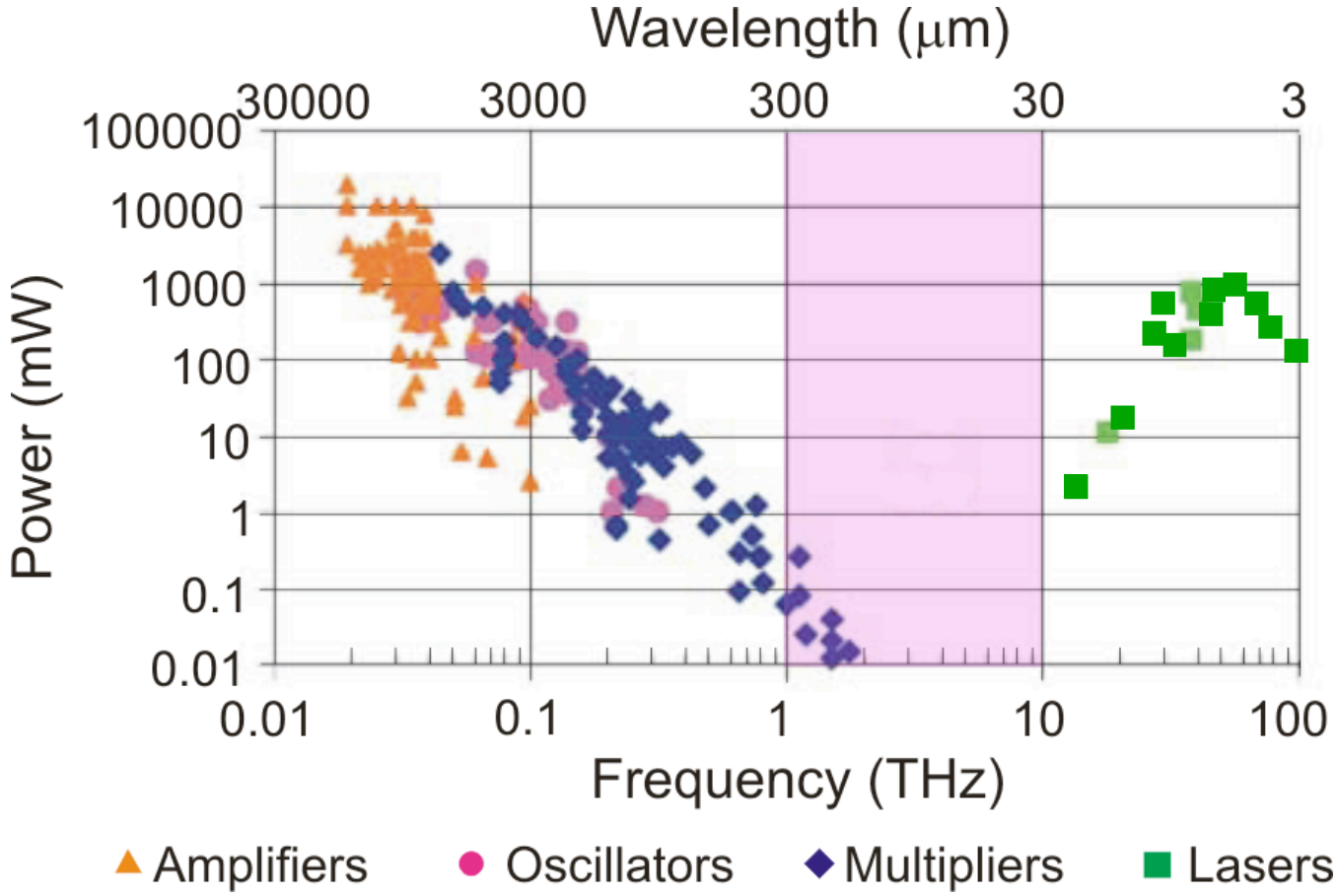


Plot adapted from: Woolard *et al. Proc. IEEE* **93**:1722 (2005),
(2005 survey of THz sources, Dr. J. Hesler, Virginia Diode Inc. )

# Origin of THz gap in semiconductor devices

Review: Generation of electromagnetic waves, back to Maxwell Eqs.

$$\nabla \times \vec{E} = -\frac{\partial \vec{B}}{\partial t},$$ sourceless, only deal with E & M wave propagation

$$\nabla \times \vec{H} = \left(\vec{J} + \frac{\partial \vec{P}}{\partial t}\right) + \varepsilon_o \frac{\partial \vec{E}}{\partial t},$$ solely responsible in generating E & M waves

$$\left.\begin{aligned} \nabla \bullet \vec{B} &\equiv 0 \\ \nabla \bullet \vec{D} &= \rho \end{aligned}\right\}$$ only responsible for static fields

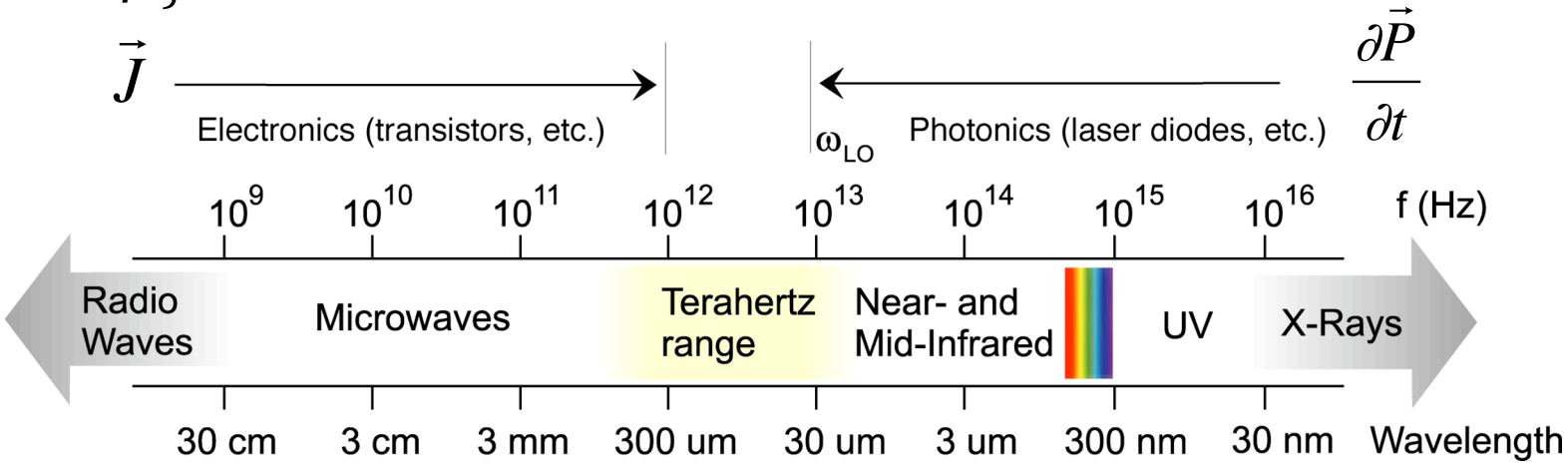


Limited by transit time and *RC*, at least two poles and $P \propto 1/f^4$.

Limited by energy gap, even for Pb-salt lasers, f > 10 THz.

# Example of a semiconductor electronic device
## — Bipolar Junction transistor (BJT)

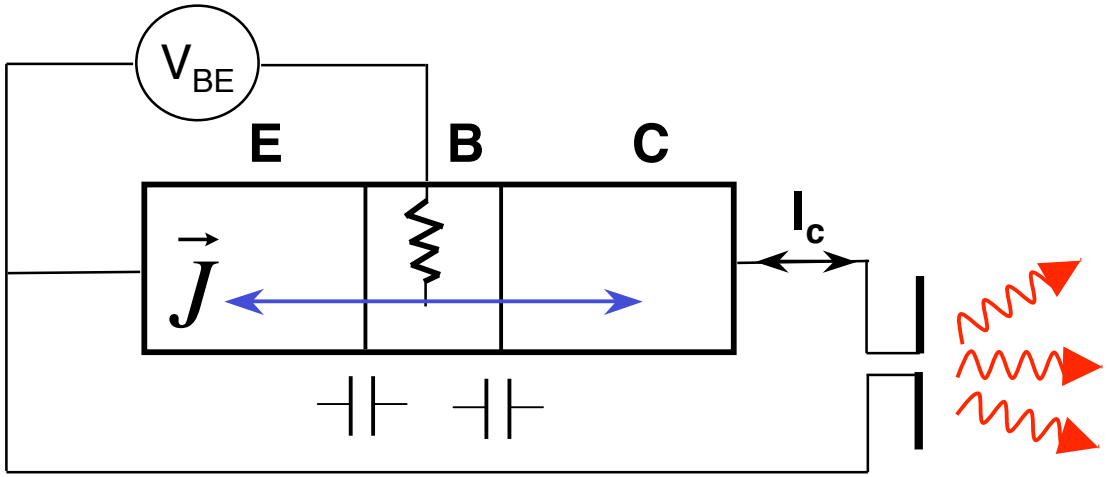


- Working principle: Applying an AC base-emitter voltage $V_{BE}$ to generate an AC collector current $I_c$ (the $J$ term).
- It takes a finite transient time $\tau_{tr}$ for electrons to travel from E to C.
- In addition, it will take a $\tau_{RC} = RC$ time to charge up unavoidable capacitors.
- Frequency response of the BJT rolls off at $f_{3dB} = 1/(2\pi\,\tau_{RC})$ or $1/(2\pi\,\tau_{tr})$. Even for $\tau \approx 200$ fs, $f_{3dB} < 1$ THz. Consequently, power drops as $1/f^4$ or faster at ≥1 THz.
- Extremely difficult to develop powerful THz electronic sources.

# Example of a semiconductor photonic device
## — Bipolar laser diode

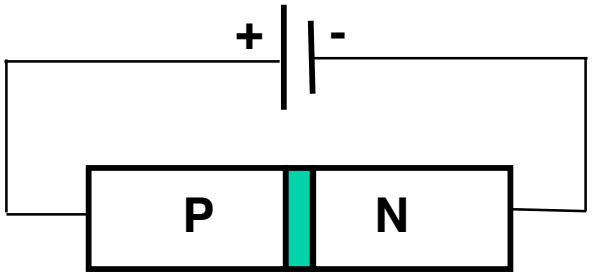


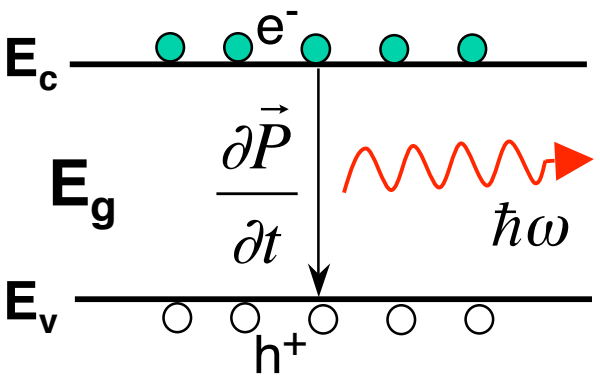


- Working principle:
  - — Applying a forward bias voltage across a *p*-*n* diode to create population inversion at the *p*-*n* junction.
  - — The *electron-hole* pairs ($e^-$-$h^+$) oscillate, generating a displacement current $\partial P/\partial t$, which produces radiation.
- Clearly, this mechanism is not limited by the transient time $\tau_{tr}$ or the *RC* roll-off at high frequencies.
- However, the photon energy $\hbar\omega$ is limited by the energy gap $E_g$, which is ≥40 meV (~10 THz) even for narrow-gap lead-salt materials.
- Hence the so-called THz gap between the conventional electronic and photonic devices.

# QCLs to the rescue

- Semiconductor quantum wells are human-made quantum mechanical systems whose energy levels can be designed to be any value. They are natural candidates to fill this technological gap.

- Quantum-cascade intersubband lasers were successfully developed in 1994 in mid-infrared frequencies ($\lambda \sim 4\ \mu$m), but it took almost 8 more years to develop the THz version because of two unique challenges for THz quantum-cascade lasers:

  — achieving a sufficient level of population inversion with narrow subband separations.
  — THz mode confinement at long wavelengths.

# Requirement to achieve THz lasing

- Lasing occurs when the modal gain $\Gamma g$ equals the total cavity loss $\alpha_W + \alpha_m$, or

$$g = \frac{\alpha_W + \alpha_m}{\Gamma}$$

$\alpha/\Gamma \sim$ 10-20 cm$^{-1}$, by using metal-metal waveguides for mode confinement.

- For intersubband transitions, because two subbands track each other in the ***k***-space, the material gain is simply given:

$$g_{peak} = \Delta n_{3D}\left(\frac{e^2\omega}{\pi\hbar\varepsilon_r^{1/2}\varepsilon_o c_o}\right)\frac{z_{ij}^2}{\Delta f} = \Delta n_{3D}\left(\frac{e^2}{2\pi\varepsilon_r^{1/2}\varepsilon_o c_o m^*}\right)\frac{f_{ij}}{\Delta f}$$

$$\approx 67\left(\Delta n_{3D}/10^{15}cm^{-3}\right)\frac{f_{ij}}{\Delta f/THz}\,cm^{-1}$$

Need a large $z_{ij}$ (or $f_{ij}$), narrow $\Delta f$, and a large $\Delta n_{3D}$ (~3×10$^{14}$/cm$^3$ ~5% of total density).

# Schematic of different intersubband emitters

- Intrawell transition.
  - Advantages: Large dipole moment, narrow linewidth.
  - Disadvantages: Challenging to implement LO-phonon-assisted depopulation of the lower lasing level.

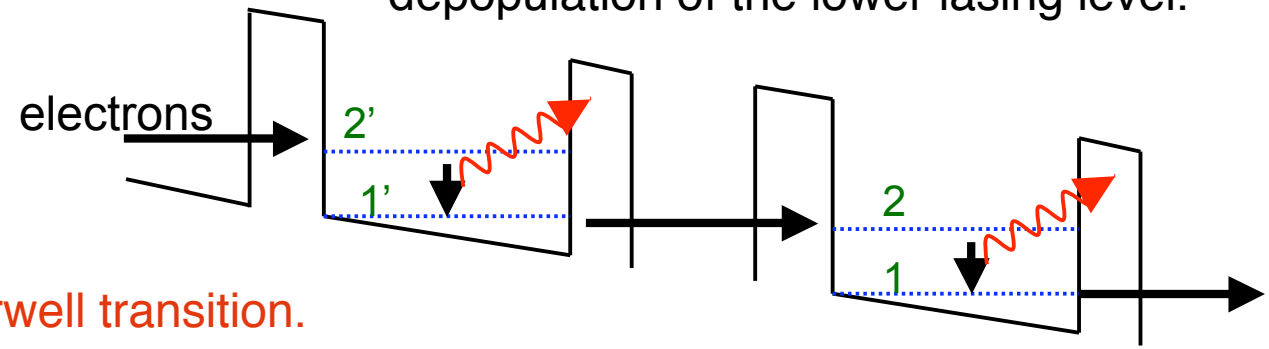


- Interwell transition.
  - Advantages: Can use fast LO-phonon scattering for depopulation, more controllable and robust at high temperatures and high current densities.

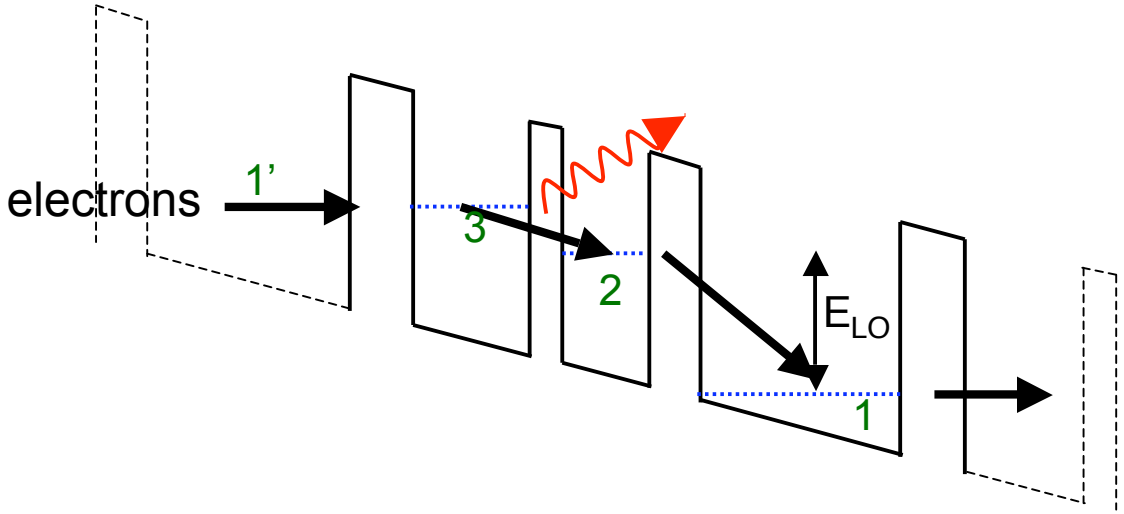

# Our first design — Diagonal transition scheme

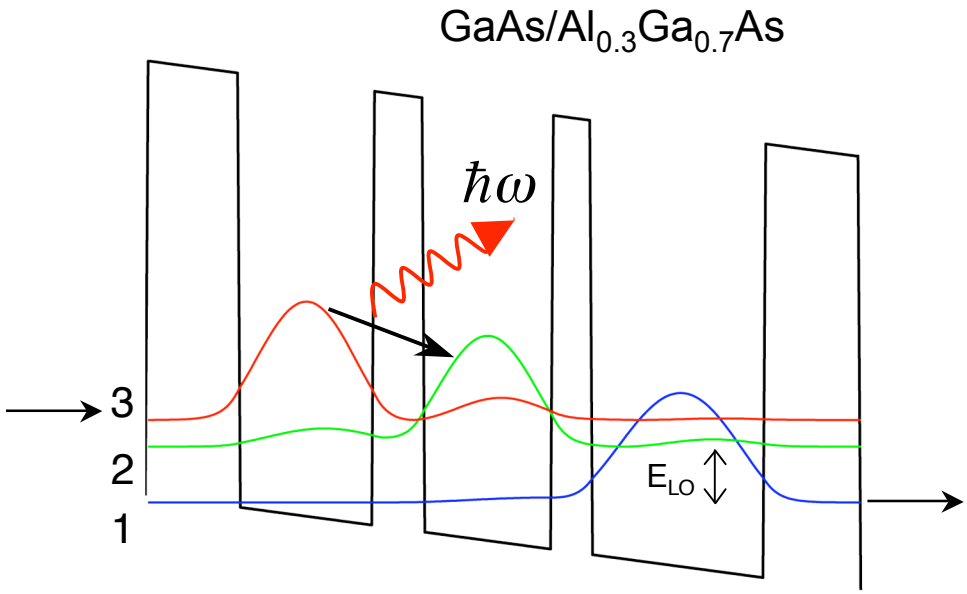


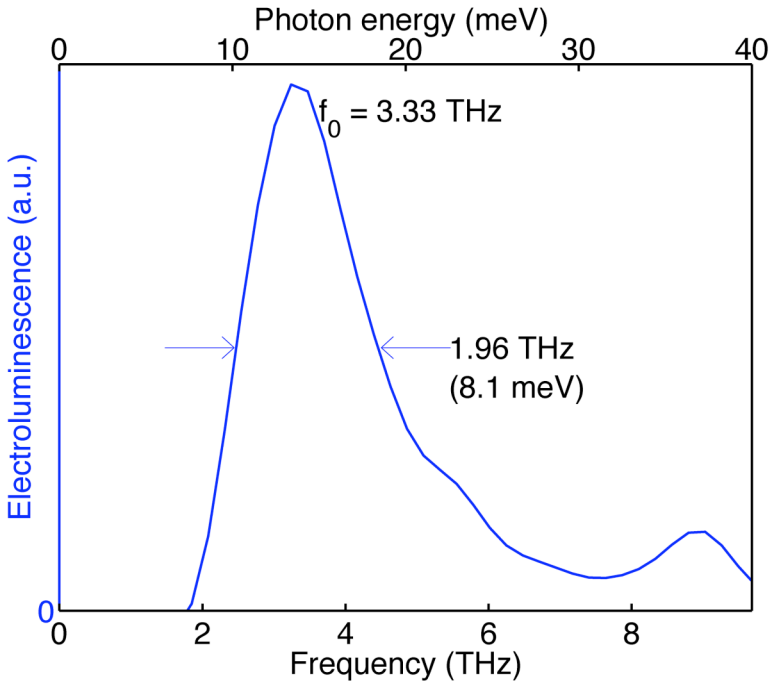


## Advantages

- Selective depopulation ($\tau_{31} >> \tau_{21}$)

B. Xu, Q. Hu, and M. R. Melloch, APL, **71**, 440 (1997).

## Disadvantages

- Small oscillator strength due to reduced overlap
- Broad linewidth due to interface roughness scattering

# Our second design — Vertical transition scheme

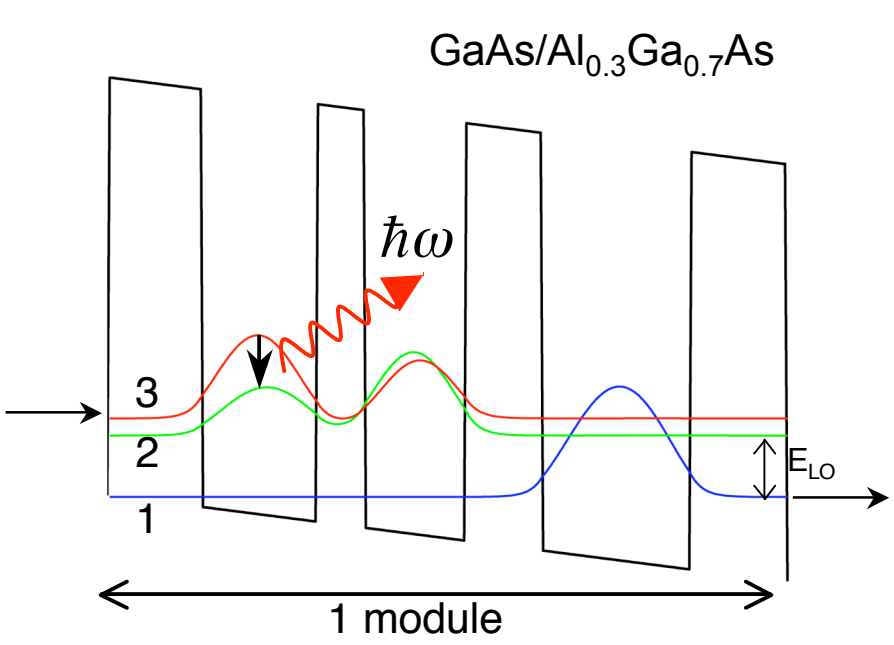


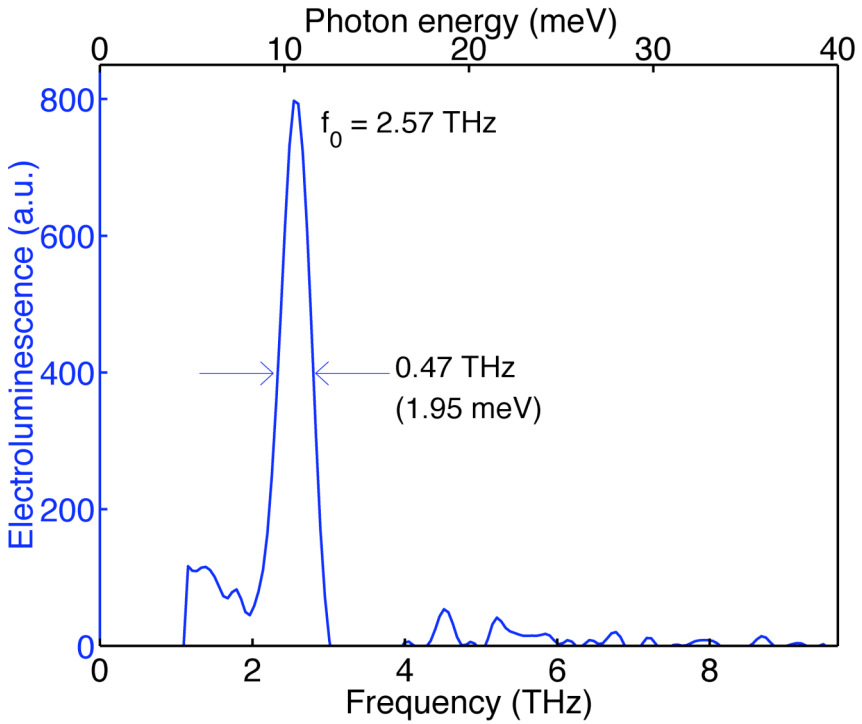


B. S. Williams, B. Xu, Q. Hu, and M. R. Melloch, APL, **75**, 2927 (1999)

## Advantages

- Larger oscillator strength
- Narrower linewidth due to reduced interface roughness scattering

## Disadvantages

- Non-selective depopulation $\tau_{31} \approx \tau_{21}$

# A parallel development — interband pumped THz intersubband lasers

H. Callebaut, MIT Master thesis (2001) unpublished

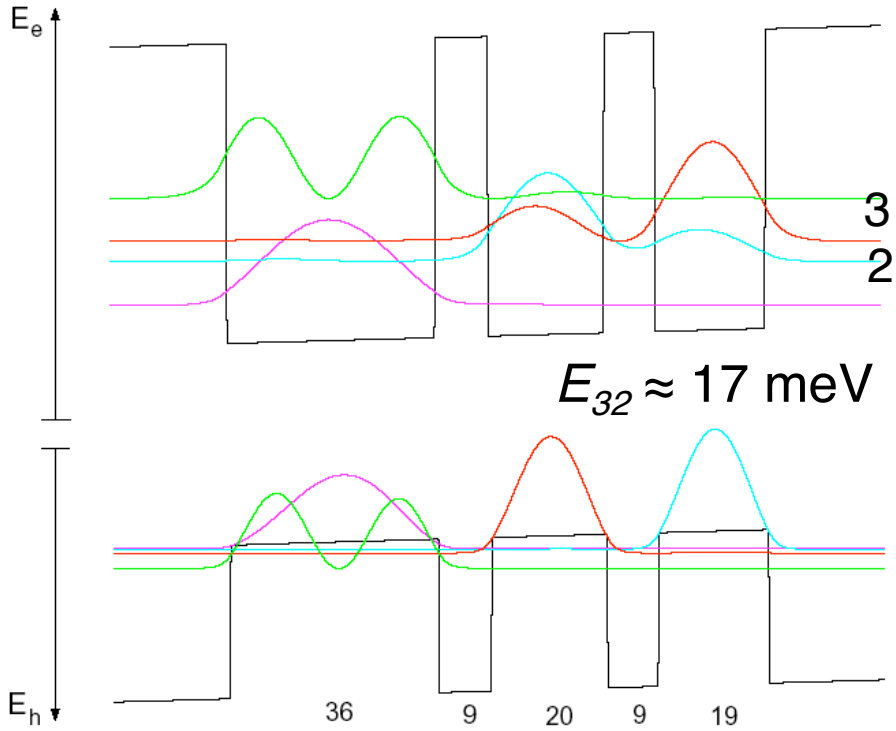


3-level design, $z_{32} \approx 36$ Å

$f_{32} \approx 0.39$

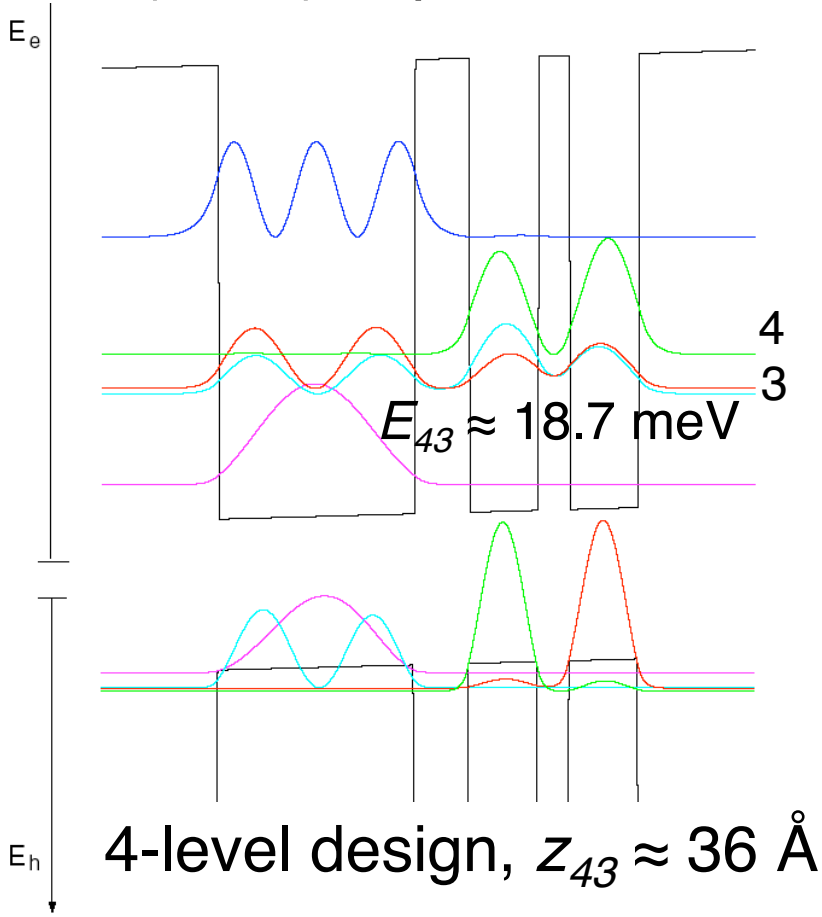


4-level design, $z_{43} \approx 36$ Å

$f_{43} \approx 0.42$

*f*-sum rule at work!

# Finally, the winning design — resonant LO-phonon scattering for depopulation

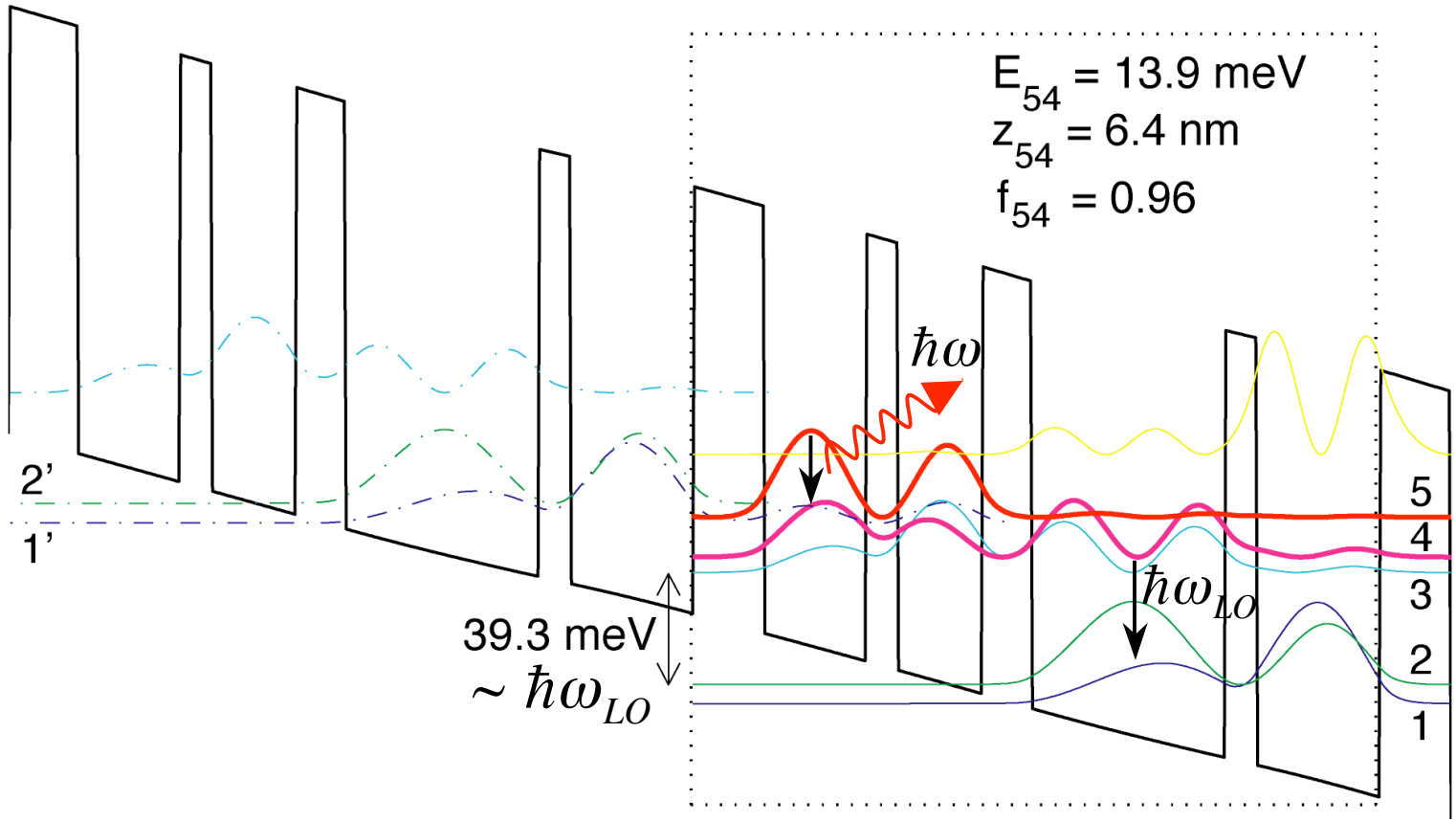


- Lasing transition is vertical between levels 5 and 4, yielding a large oscillator strength of $f_{54} \approx 0.96$.
- At the designed bias, level 4 is at resonance with level 3, enabling a very fast ($\tau_4 \approx \tau_3 \sim 0.5$ ps) depopulation scattering, while keeping the upper level's lifetime relatively long ($\tau_{5\to 2,1} \approx 7$ ps).

# First resonant phonon THz QCL (3.4 THz)

(Nov. 2002)

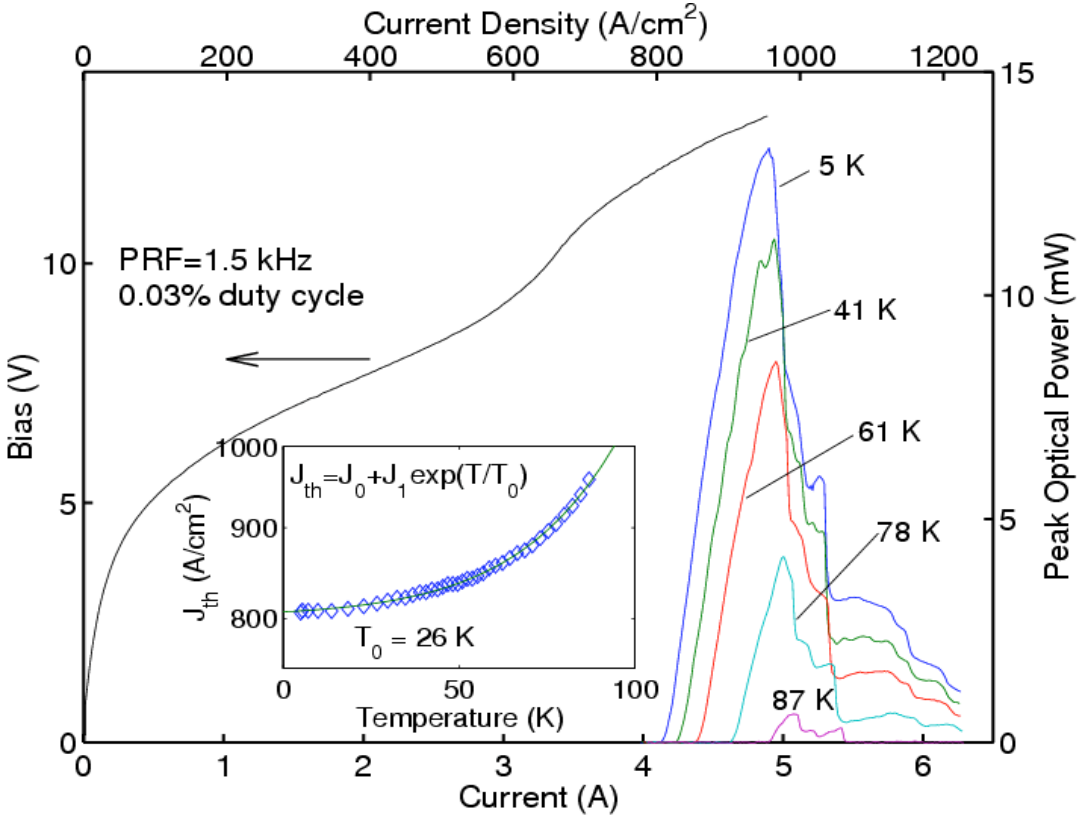


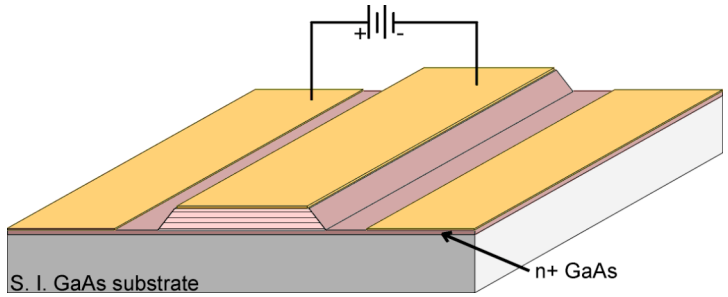


SI-surface-plasmon waveguide

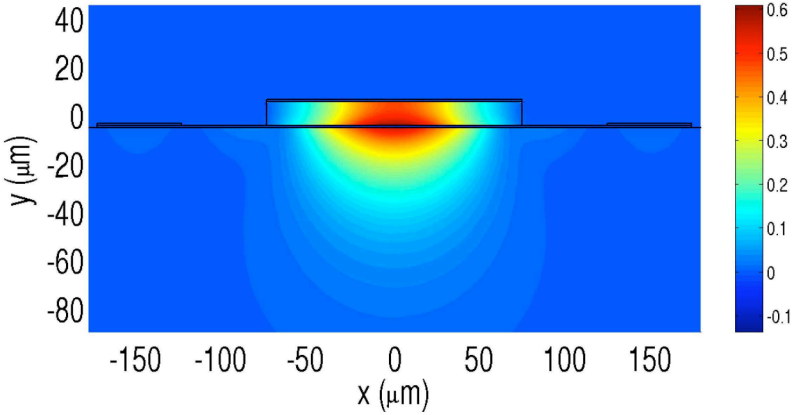


Pulsed $T_{max}$ = 87 K

Williams *et al.* APL **82**,1015 (2003)
Williams *et al.* EL **39**, 915 (2003)

# Metal-metal waveguide structure for THz mode confinement

(B. S. Williams, *et al.* APL, **83**. 2124 (2003))

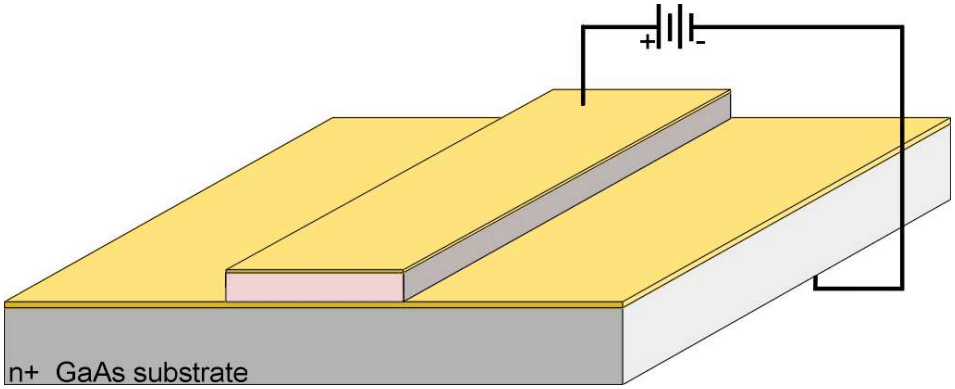


**Schematic**

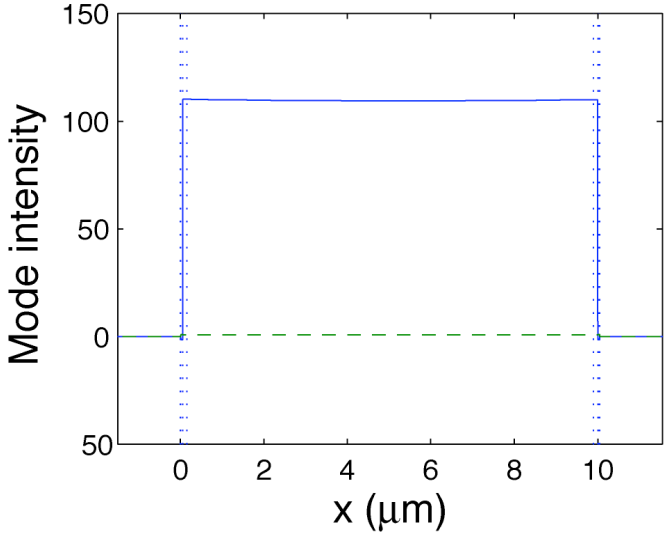


**Mode profile**

- A large confinement factor ($\Gamma \approx 98\%$) and a higher facet reflection, yielding a low threshold $\alpha/\Gamma$, and higher operating temperatures. This is especially important at longer wavelengths (>150 $\mu$m).
- Can use thinner, narrower, and shorter laser bars, allowing lateral heat removal.
- $\kappa_{metal} > \kappa_{GaAs}$ at > 100 K.
- Lessen the need for HR facet coating, a primary failure spot.

# Cu-Cu thermocompression wafer bonding

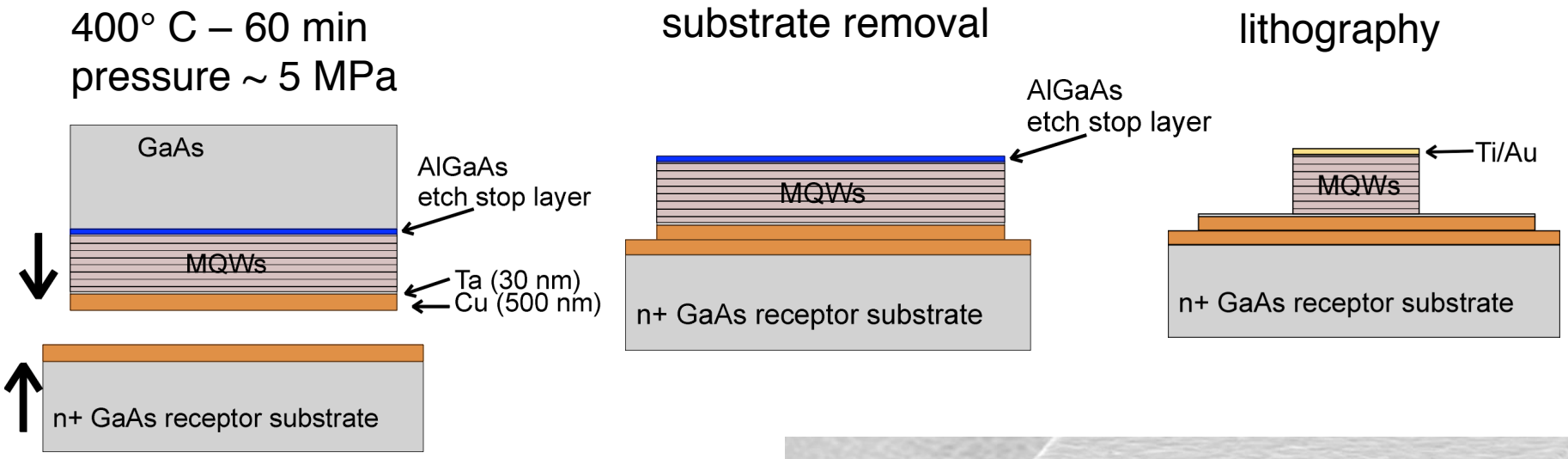


- Copper — good thermal/electrical conductivity.
- Improved bond quality and stability.
- Fabrication more difficult and requires very clean interface.

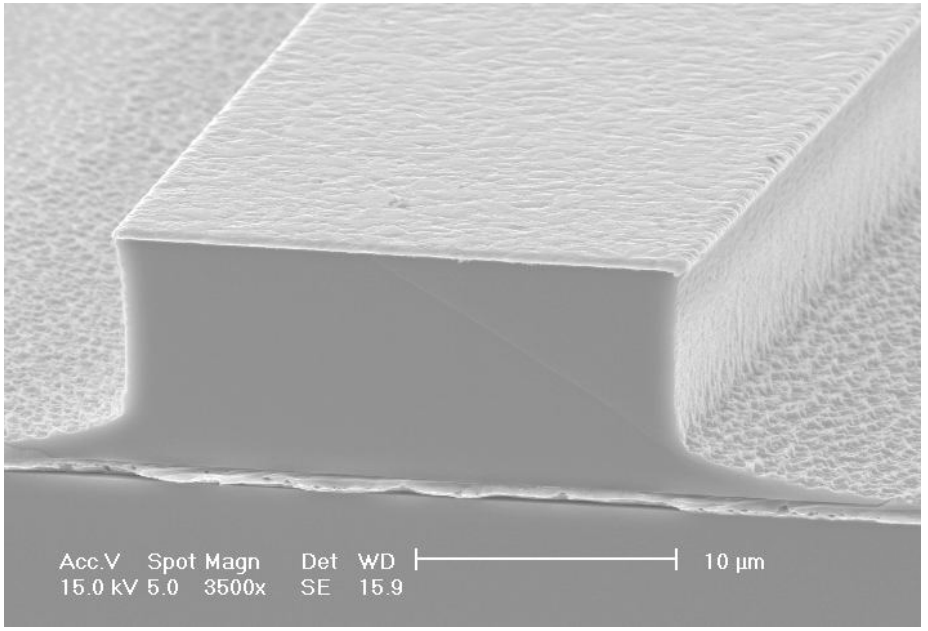

# New device with improved temperature performance

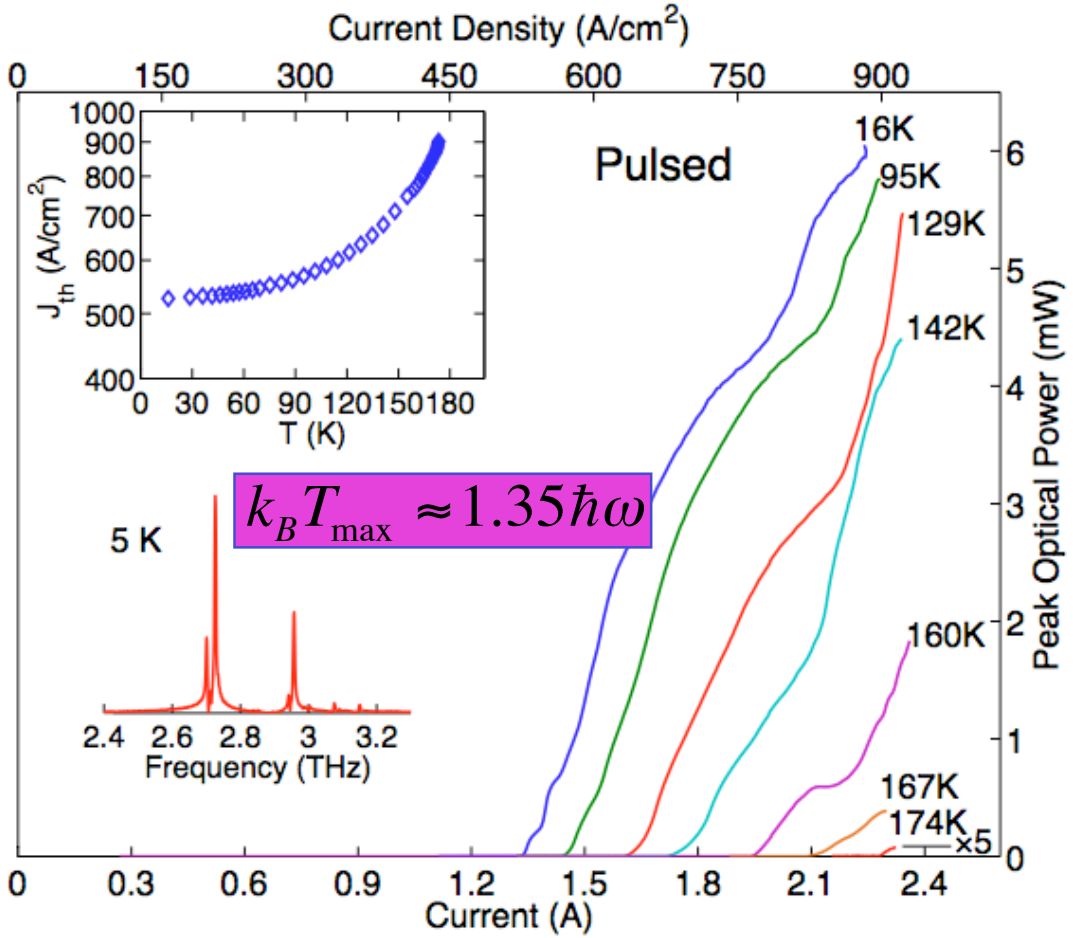


- The maximum operating temperature is $T_{max} \approx 174$ K. At this temperature, $k_B T_{max} / \hbar\omega > 1$ at 2.7 THz. This result, and results from several other THz QCL groups, are unprecedented for any solid-state photonic devices.

# CW operation up to 117 K

from a 23-μm ×1.22-mm ridge metal-metal waveguide

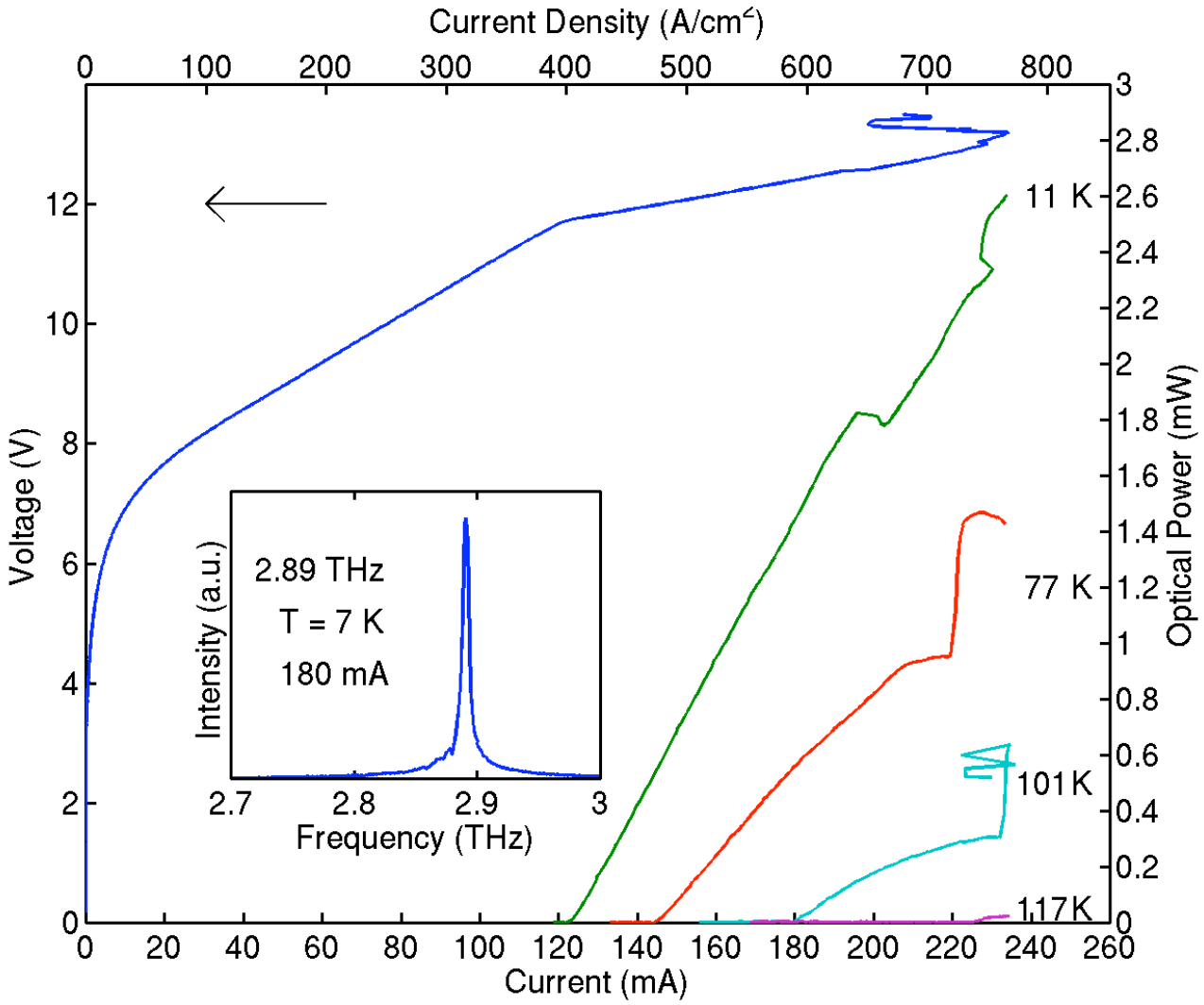


- Metal-metal waveguide fabricated with Cu-Cu bonding.
- Narrowest width/$\lambda_o$ (~0.22) of any laser, a "wire laser".
- CW threshold current ~120 mA, and power dissipation ~ 1.5 W.
- Even at 77 K, still >1 mW of power.

(Opt. Express **13**, 3331 (2005)).

# New design for longer-wavelength QCLs

(S. Kumar *et al.* APL **88**, 121123 (2006))

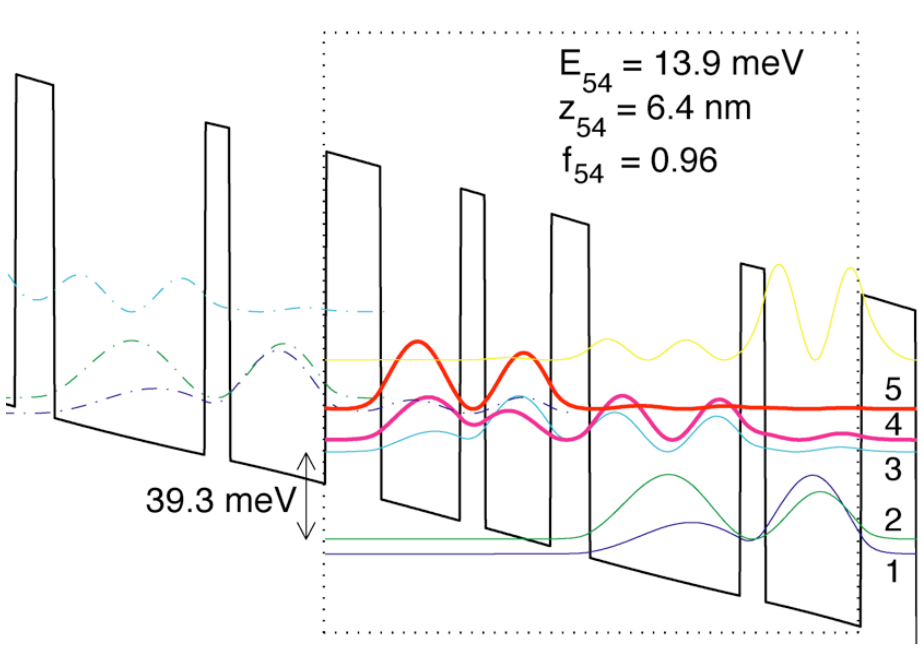


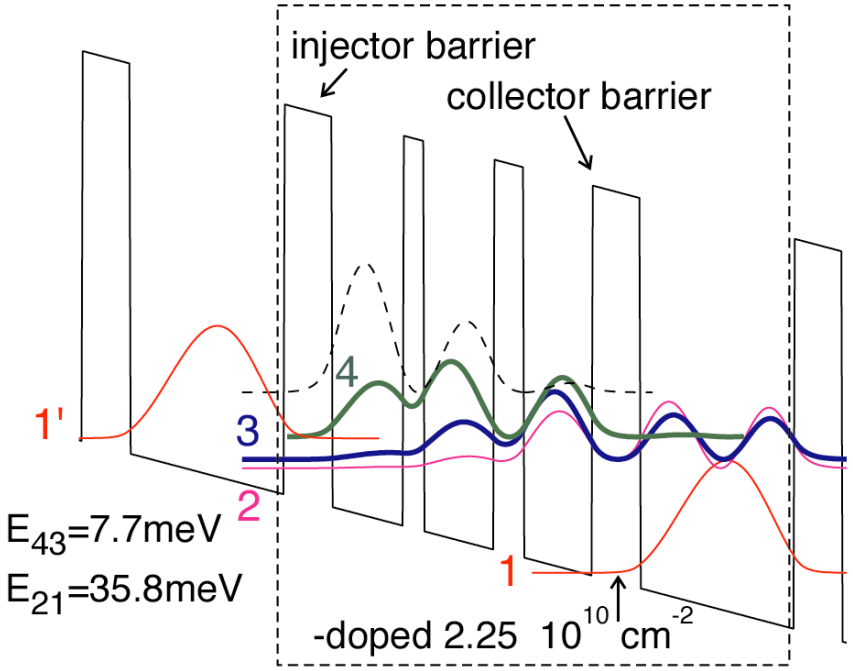


Previous design has two (or more) levels in the injector region ($E_1$ and $E_2$). Absorption between $E_1$ and $E_2$ can be significant at lower frequencies ($E_2$-$E_1$ ≈ 1.3 THz).

The new design has only one level in the injector region ($E_1$), largely eliminating this reabsorption problem.

# New one-well design for longer-wavelength QCLs

(S. Kumar *et al.* APL **88**, 121123 (2006))

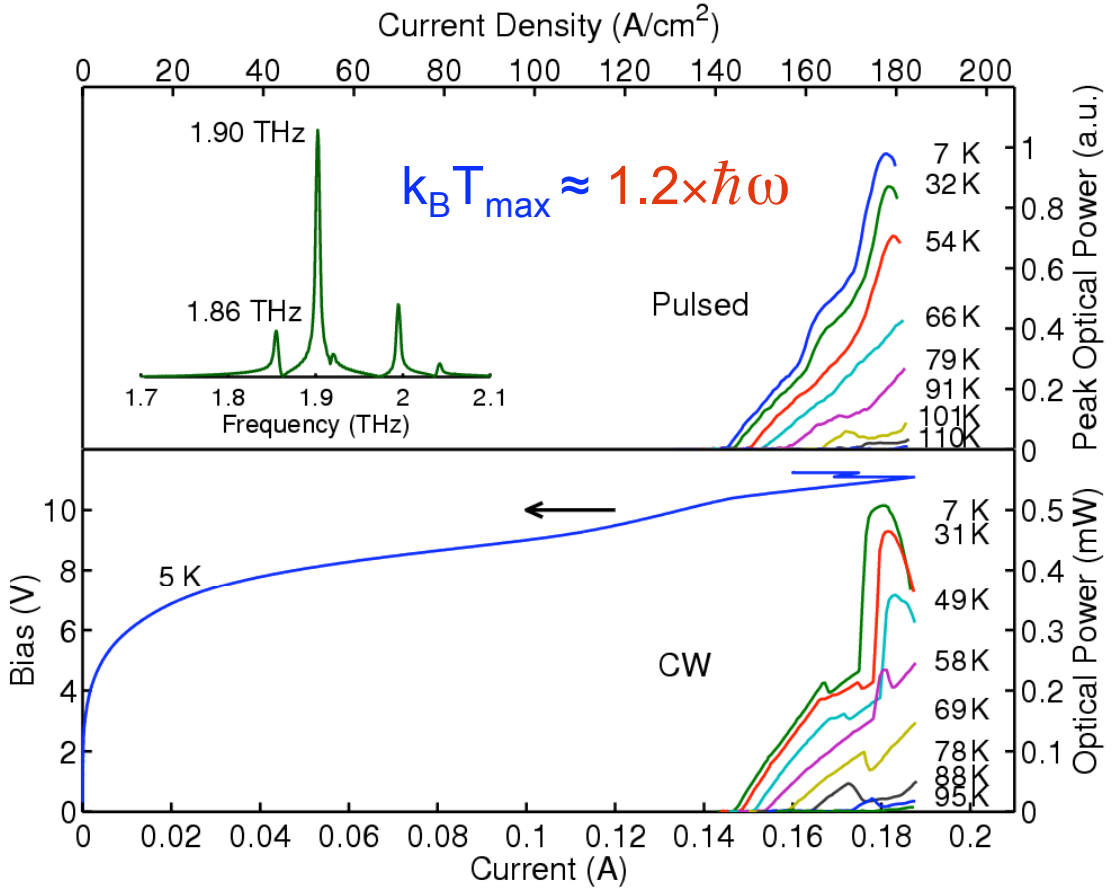


- $J_{th} \sim 140$ A/cm$^2$, the lowest of resonant-phonon THz QCLs, validating low waveguide losses.

# Long-wavelength QCL based on the one-well design

(S. Kumar *et al.* (2007))

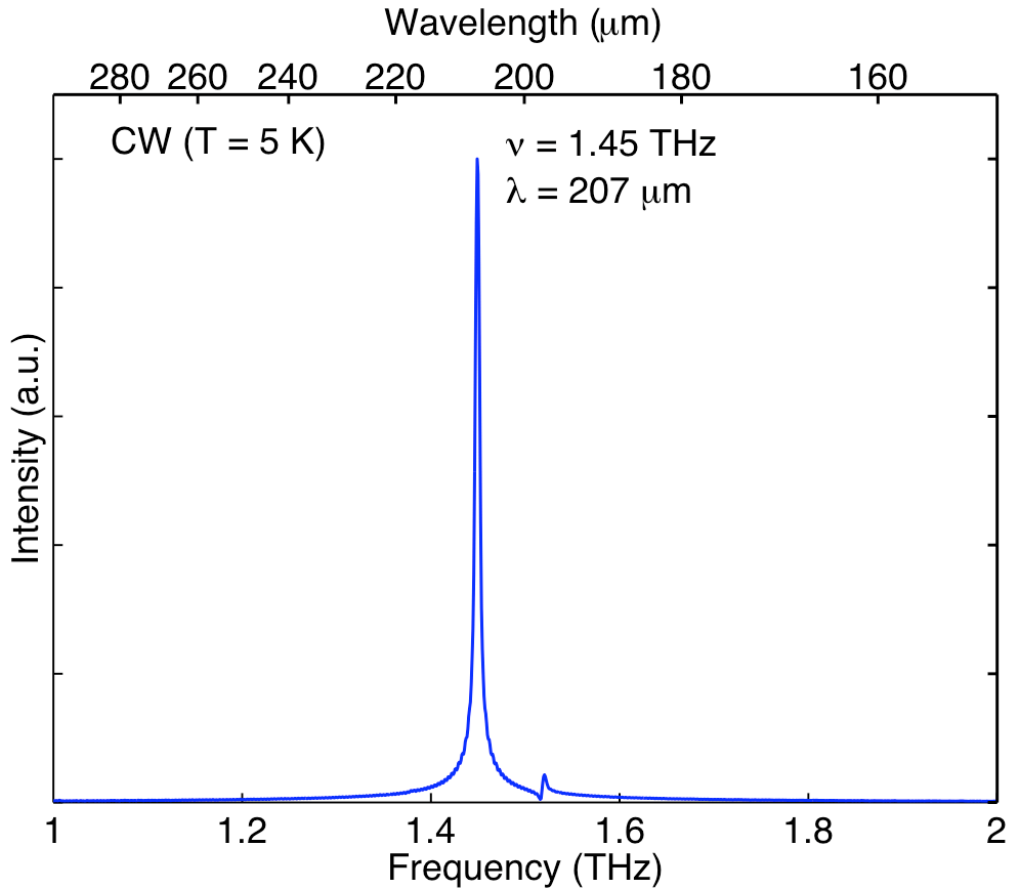


- Have achieved lasing at ~1.45 THz, corresponding to $\lambda \approx 207\ \mu m$.

# Sub-THz QC lasers with magnetic field

(A. Wade et al. submitted (2008))

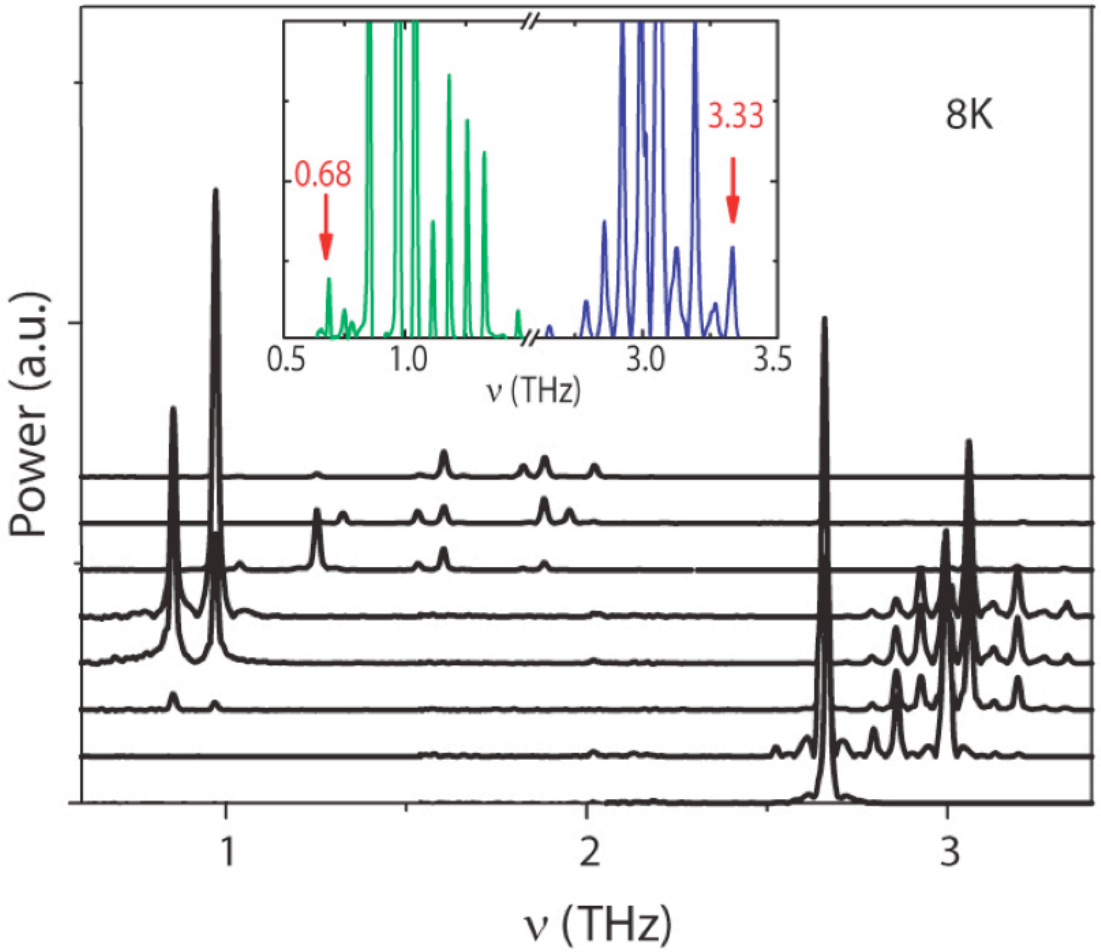


- Lasing at ~0.68 THz, corresponding to $\lambda \approx 440\ \mu m$.
- The same device lased from 0.68 THz to 3.3 THz.

# 0.6-THz QC lasers with magnetic field

(A. Wade et al. (2008))

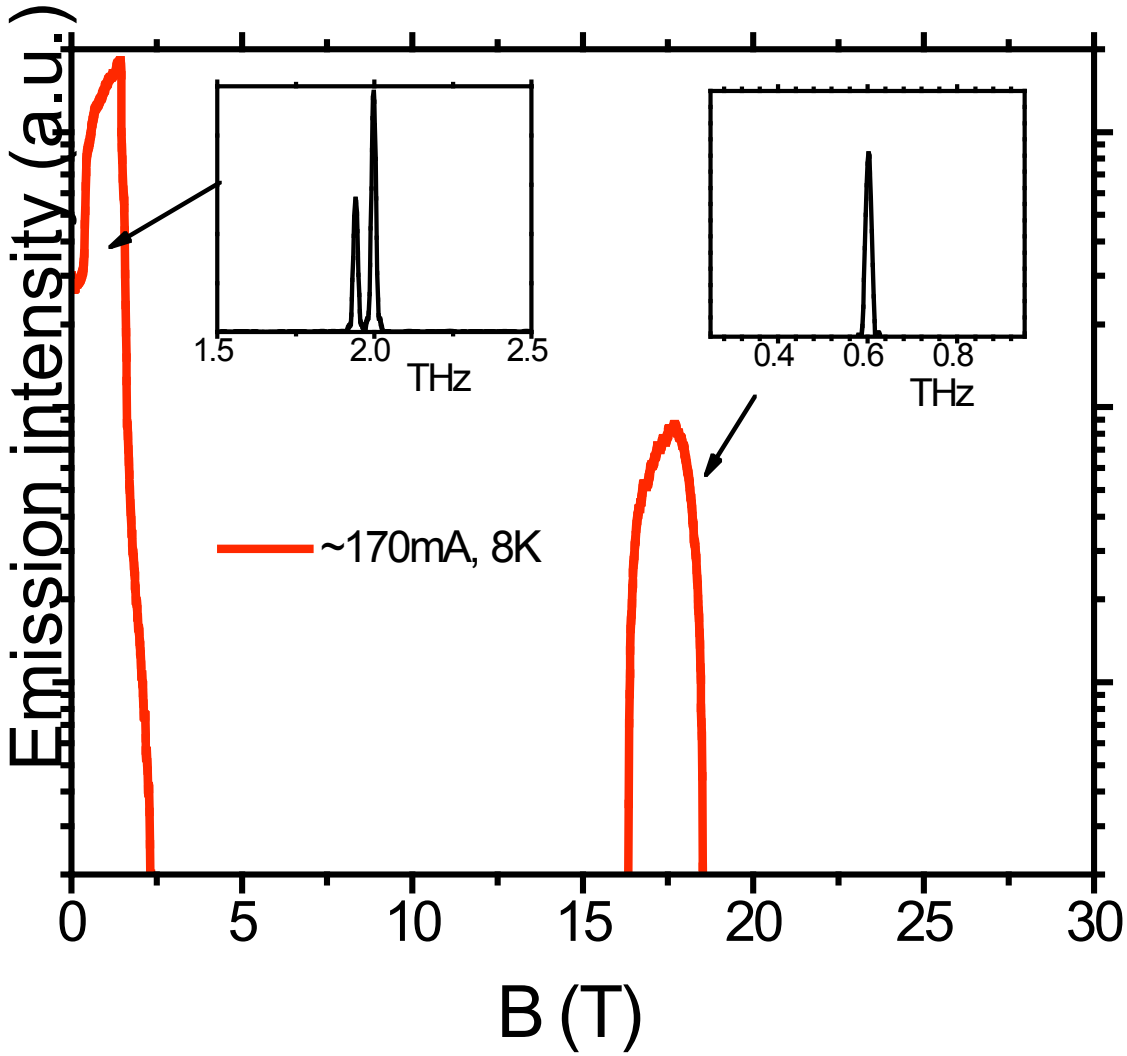


From a 1.9-THz QCL based on one-well injector. Kumar *et al.* APL (2006)

# High-temperature THz QC lasers with magnetic field

(A. Wade et al. submitted (2008))

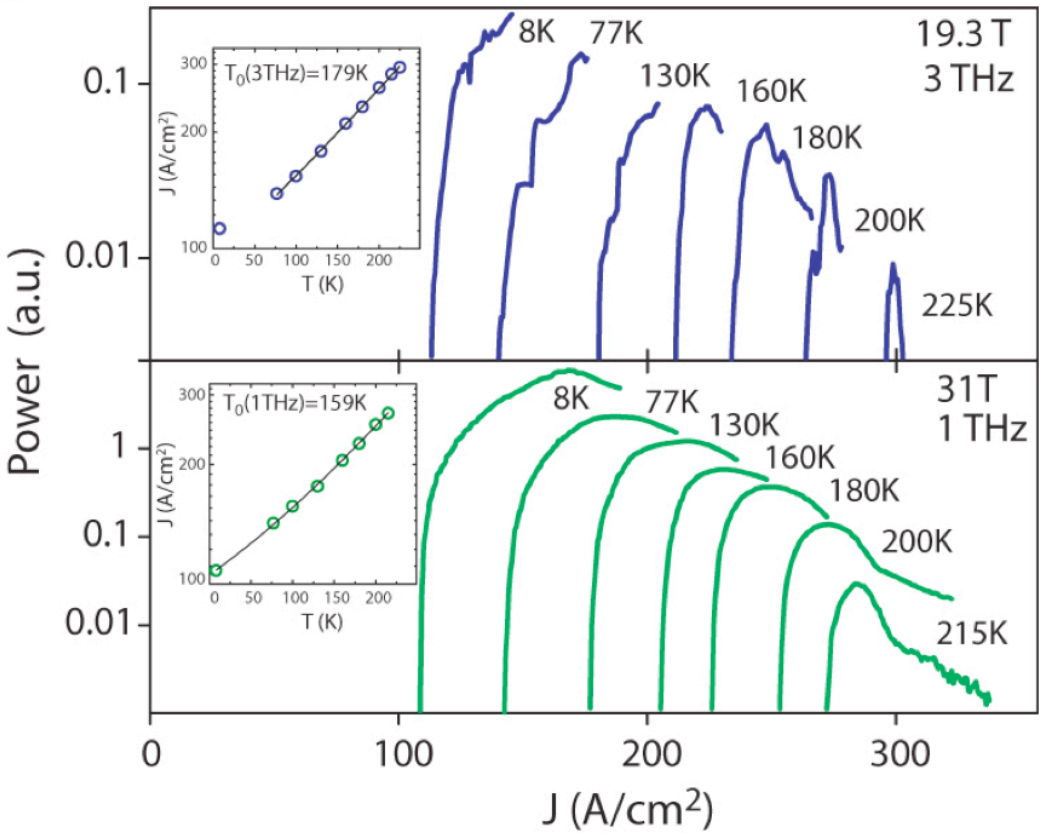


- Lasing up to ~225 K, very encouraging results, likely due to an increased upper-state lifetime.

# A 2.8-THz heterodyne receiver using a QCL as the local oscillator (LO)

(Gao *et al*. APL **86**, 244104 (2005))

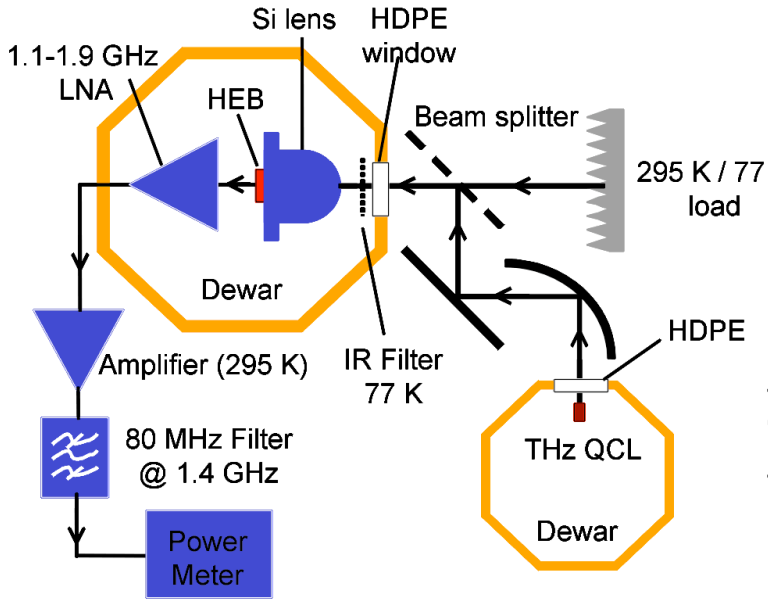


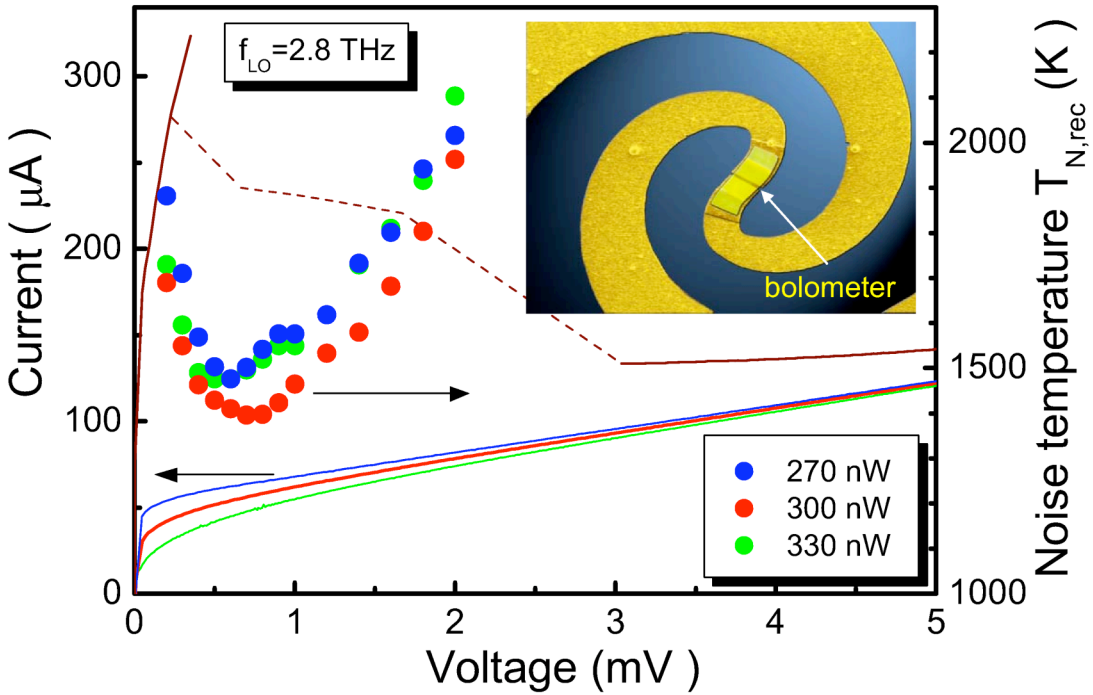


- $T_{rec} \approx 1400$ K at this high frequency (~2.8 THz).

# A frequency locked THz QCL

(Betz *et al.*, Opt. lett. **30**, 1837 (2005))

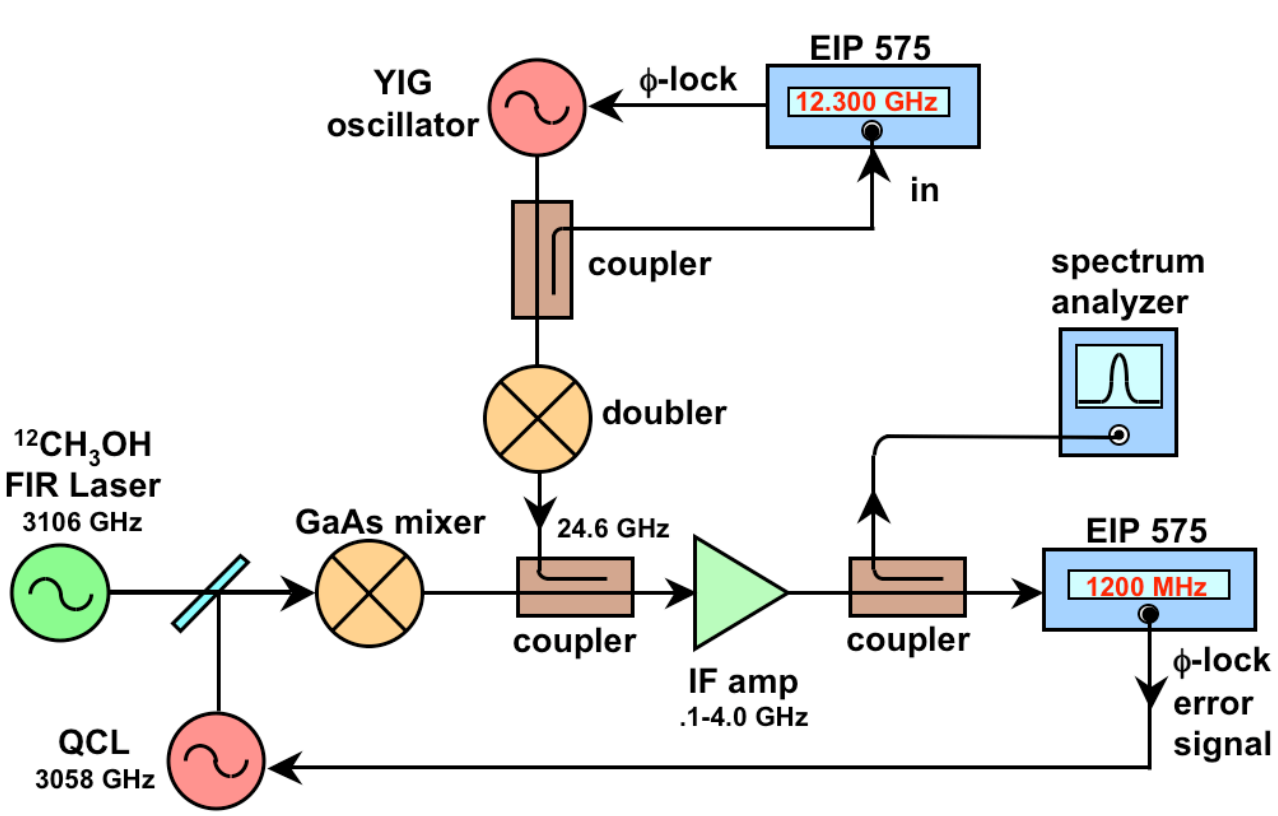


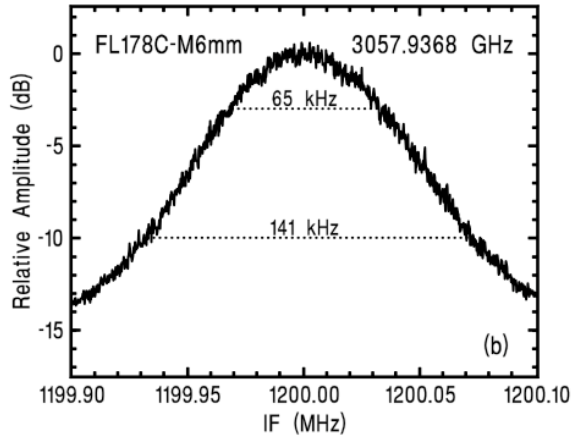


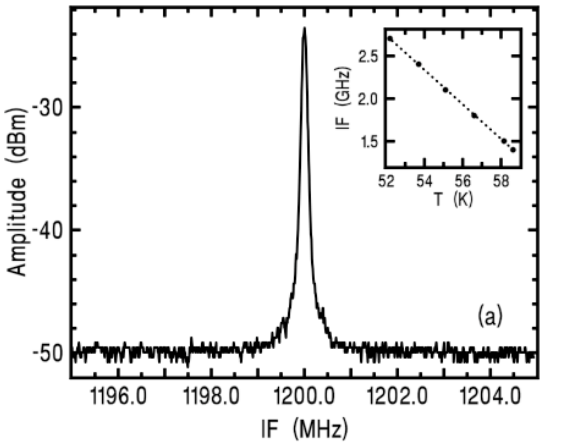


- $\Delta f$ (FWHM) ≈ 65 kHz is achieved indefinitely through frequency locking.

# A high-power QCL at ~4.4 THz

(B. S. Williams *et al.* Electr. Lett. **42**, 89 (2006))

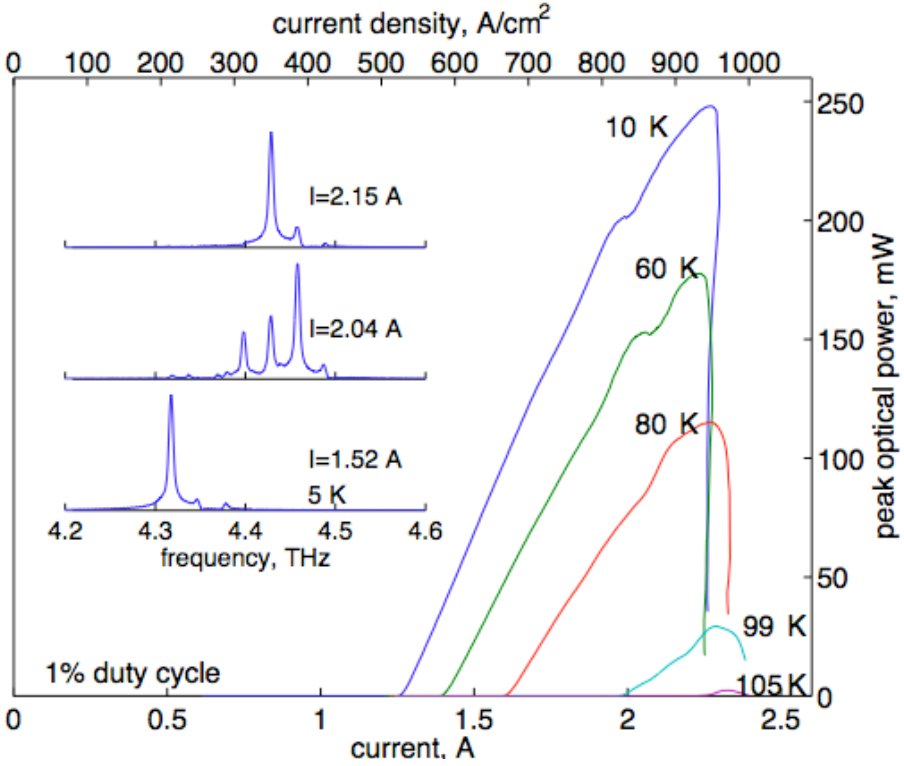


198 $\mu$m × 1.21 mm ridge

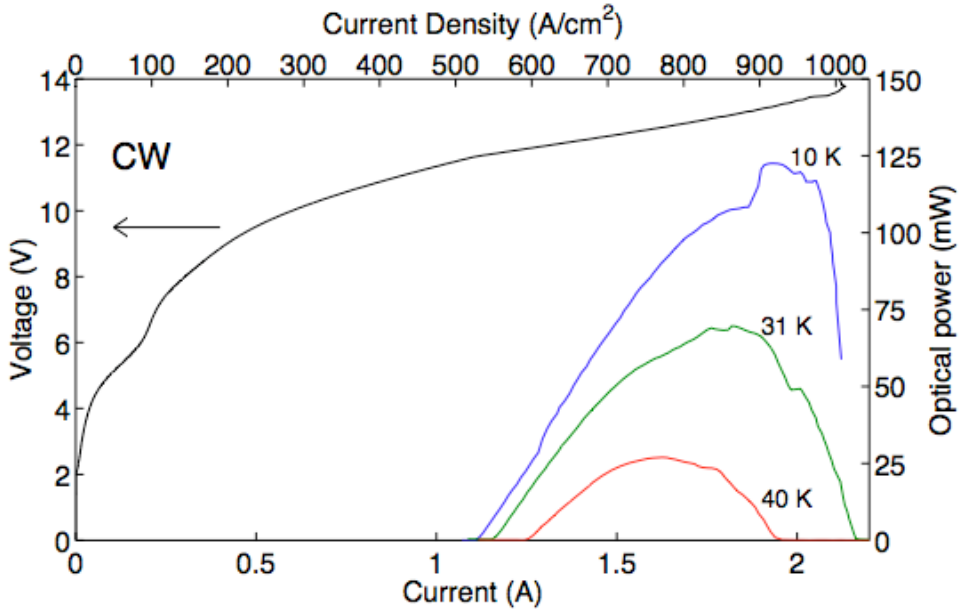


98 $\mu$m × 2.15 mm ridge

- $P_{max}$ ≈ 248 mW (pulsed) and 138 mW (CW).
- ~50 mW of CW power at pulsed-tube cooler temperature (~30 K), T-rays movies possible.

# Physical comparison between a THz QCL and a FIR gas laser

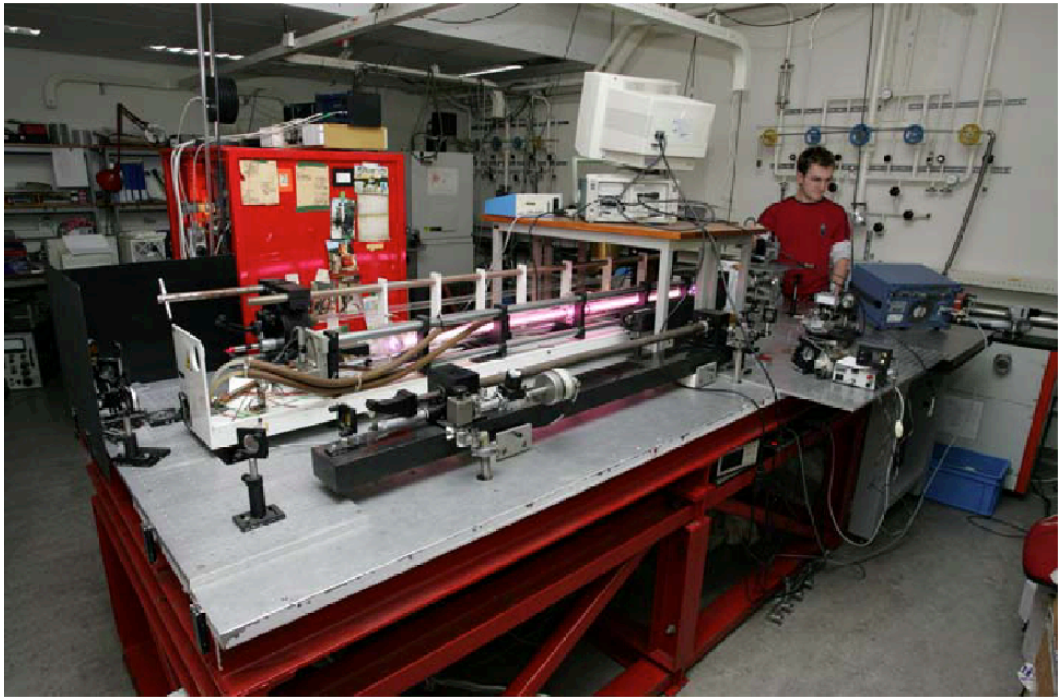

far-infrared Gas Lasers

discrete frequencies, not tunable,
large, power hungry, expensive

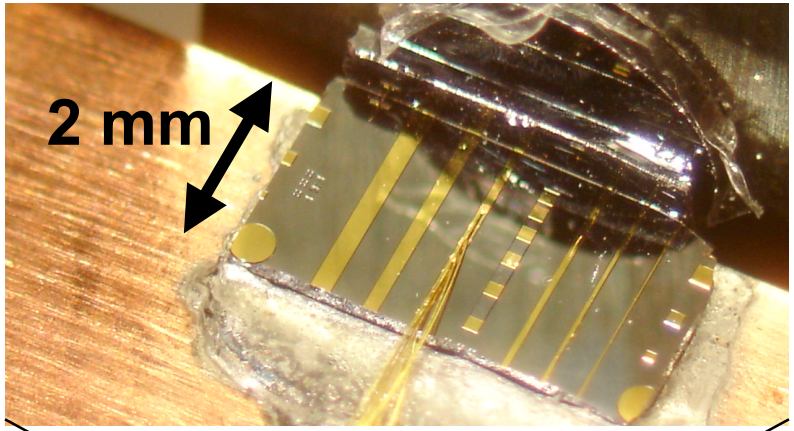


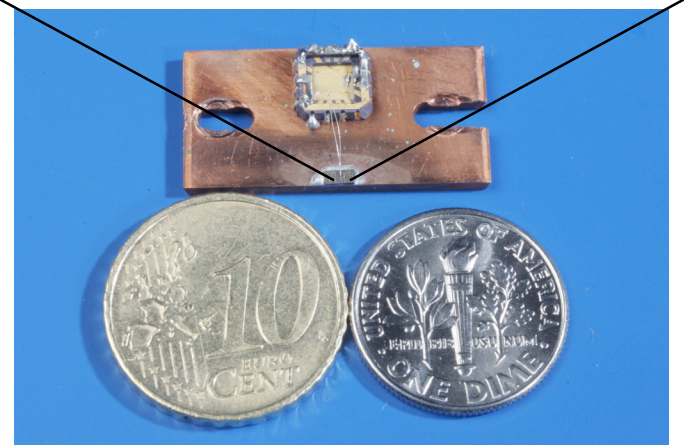


THz QCLS

more powerful, covers all
the frequencies, ...

# Waveguides for THz quantum-cascade lasers

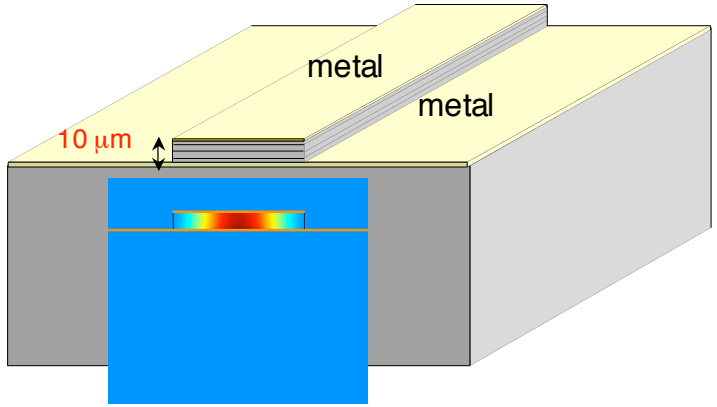


Metal-metal (MM) waveguide

## Advantages:

High mode confinement factor, and thus lower threshold and higher operating temperatures.

## Disadvantages:

Low output power and divergent beam patterns.

---

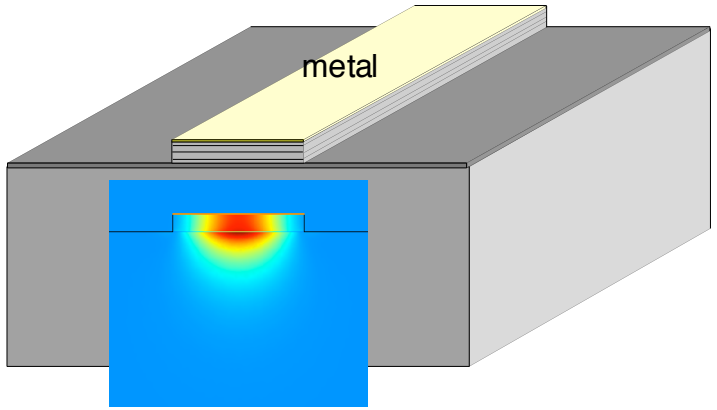


Semi-insulating surface-plasmon (SISP) waveguide

## Advantages:

High output power and narrower beam patterns.

## Disadvantages:

Higher thresholds (due to loss in the substrate) and thus lower operating temperatures.

# Recent development on high-power metal waveguide THz quantum-cascade lasers

- First approach —— Surface-emitting THz QCLs using 2nd-order DFB grating

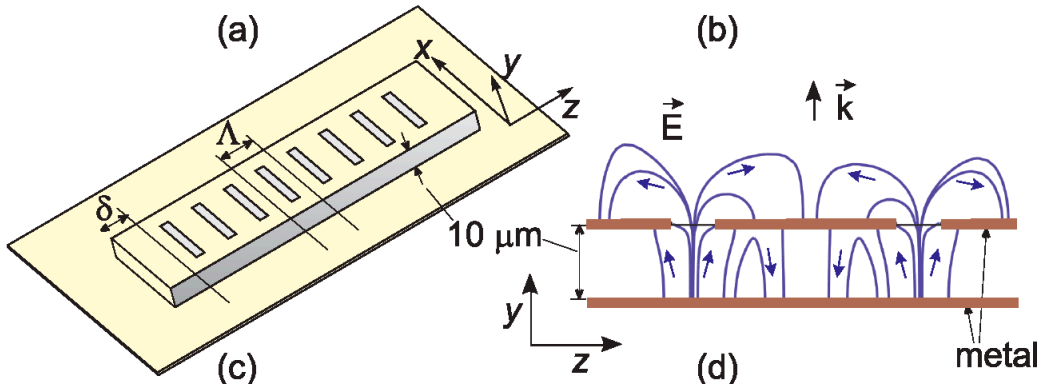


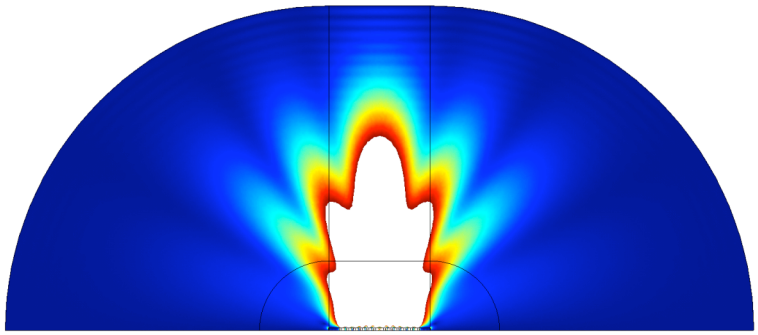

## Advantages:

- Much better beam patterns,
- higher output power levels,
- DFB in nature, single-mode operations.

# Surface-emitting THz QCLs using 2nd-order DFB grating

(S. Kumar *et al.* Optics Express **15**, 113 (2007))

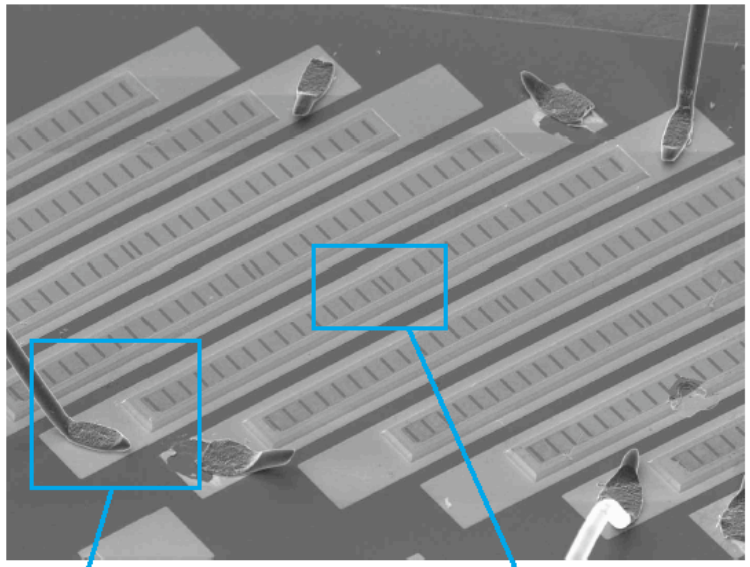

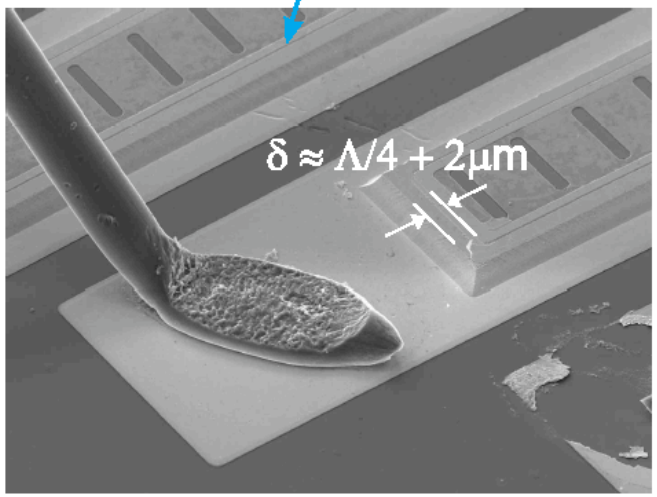


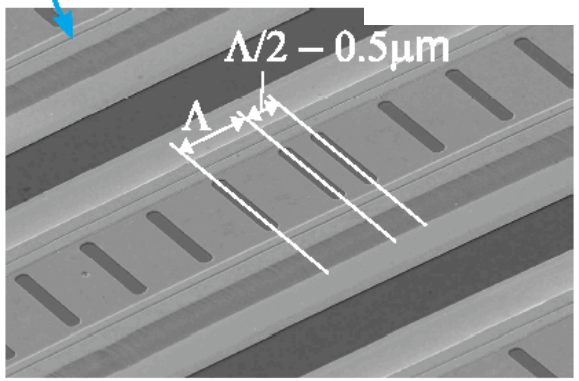


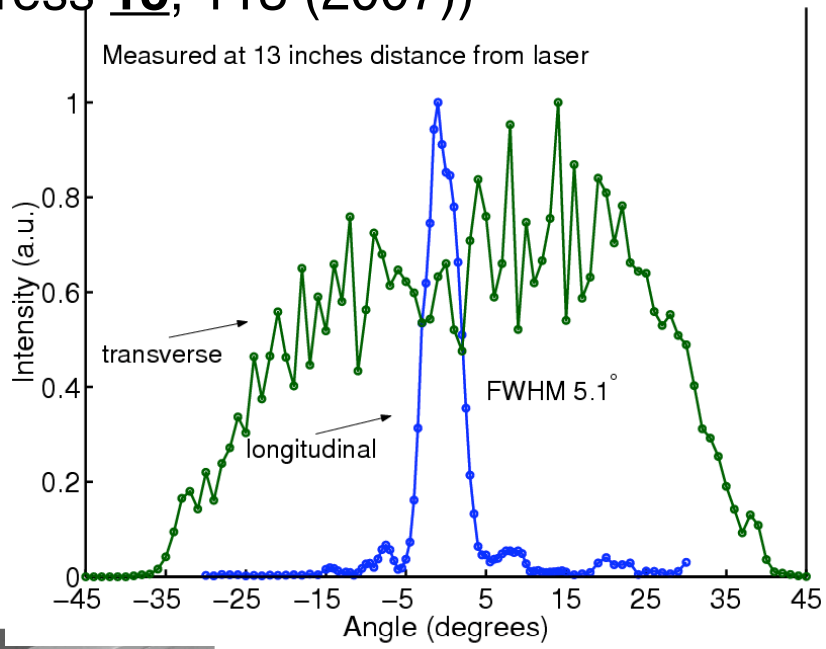


- Challenging to eliminate higher-order lateral modes.
- Facet and defect lengths are important for output beam and power levels.

# Surface-emitting THz QCLs

(S. Kumar *et al.* Optics Express **15**, 113 (2007))

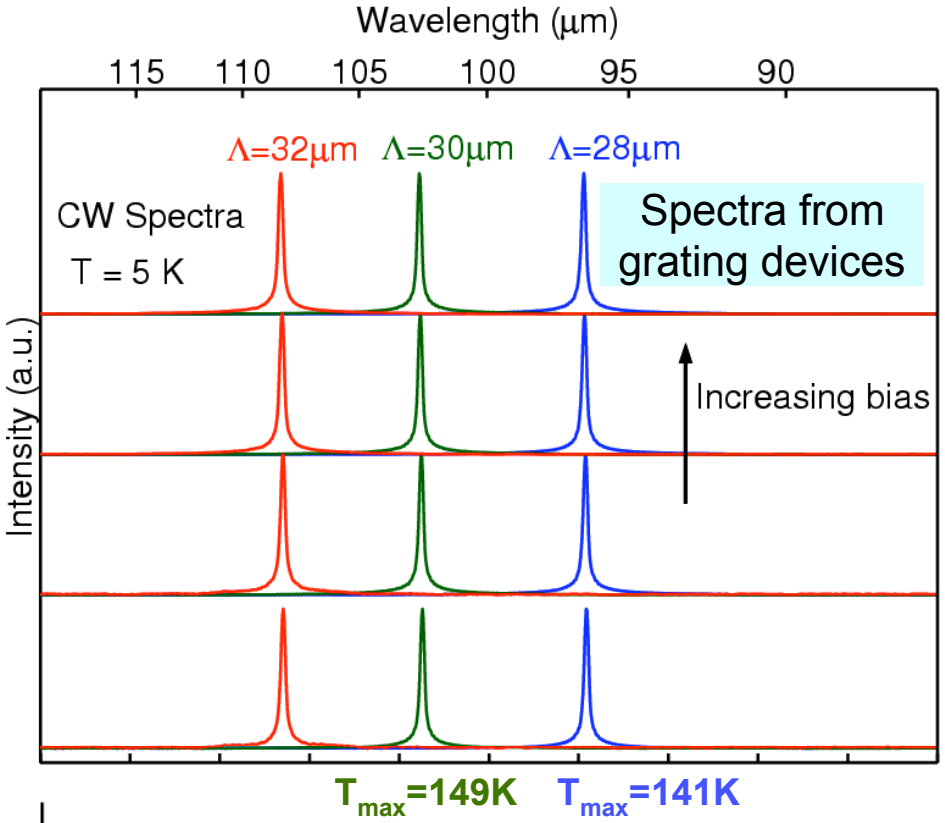


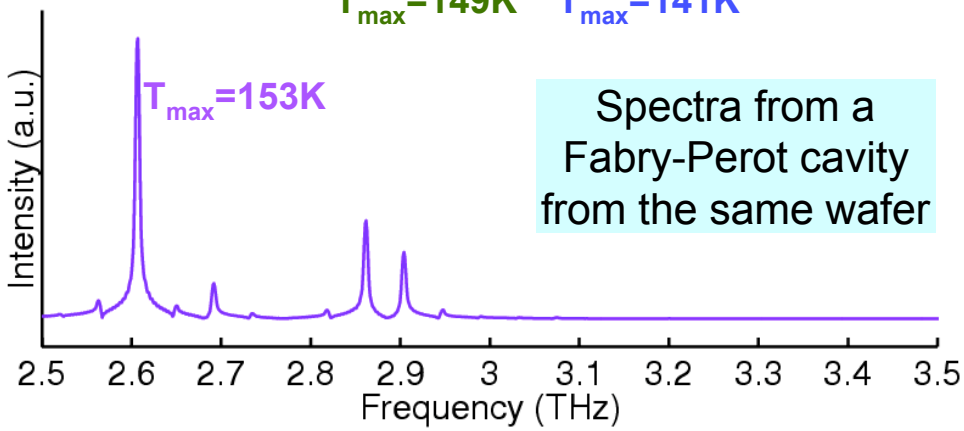


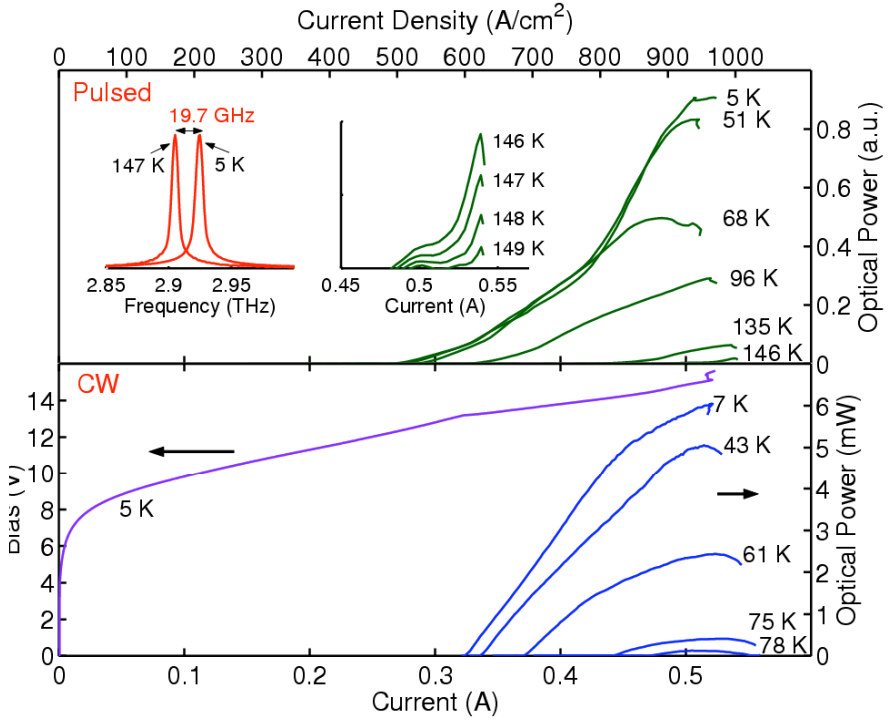


- Higher output power levels,
- robust single-mode operations,
- lasing over >0.35 THz,
- temperature tuning of ~20 GHz,
- only marginally lower maximum temperatures.

# Recent development on high-power metal waveguide THz quantum-cascade lasers (cont.)

- Second approach — lens-coupled metal-metal waveguides

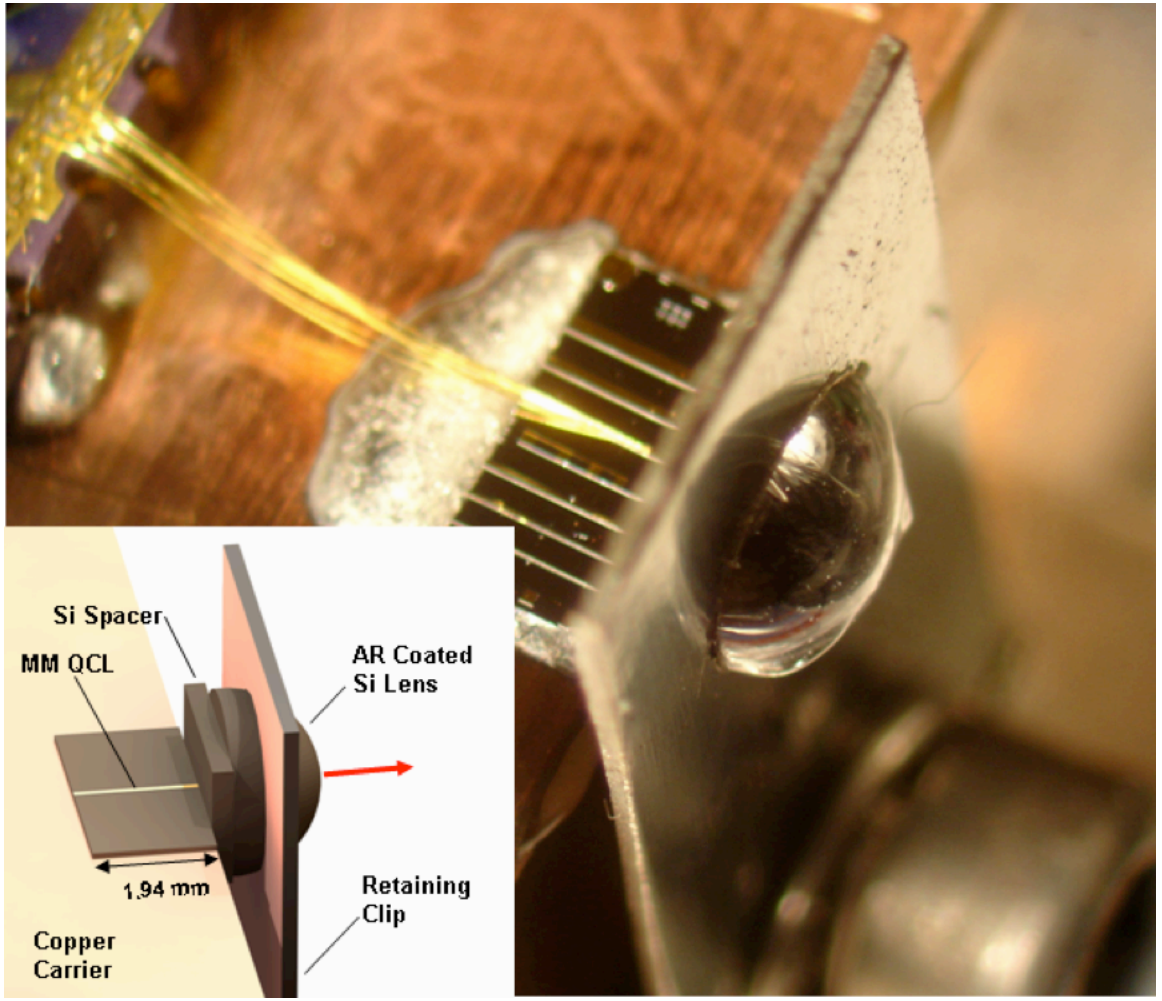


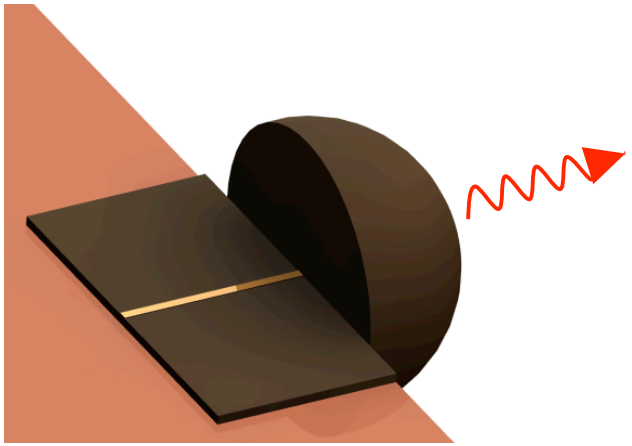

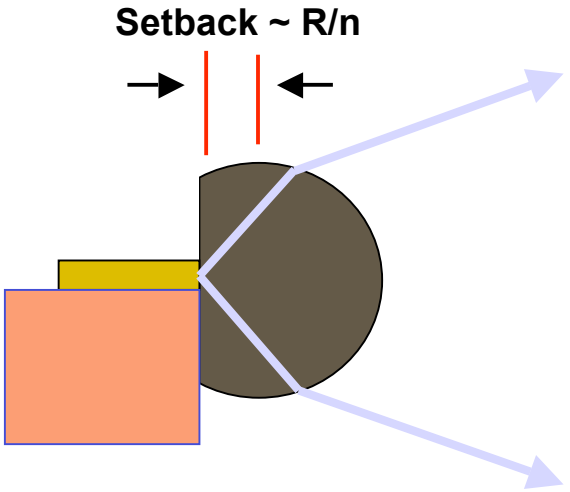

# Lens-coupled high-power metal waveguide THz QCLs

(Alan Lee *et al*. Optics Letters, **32**, 2840 (2007))

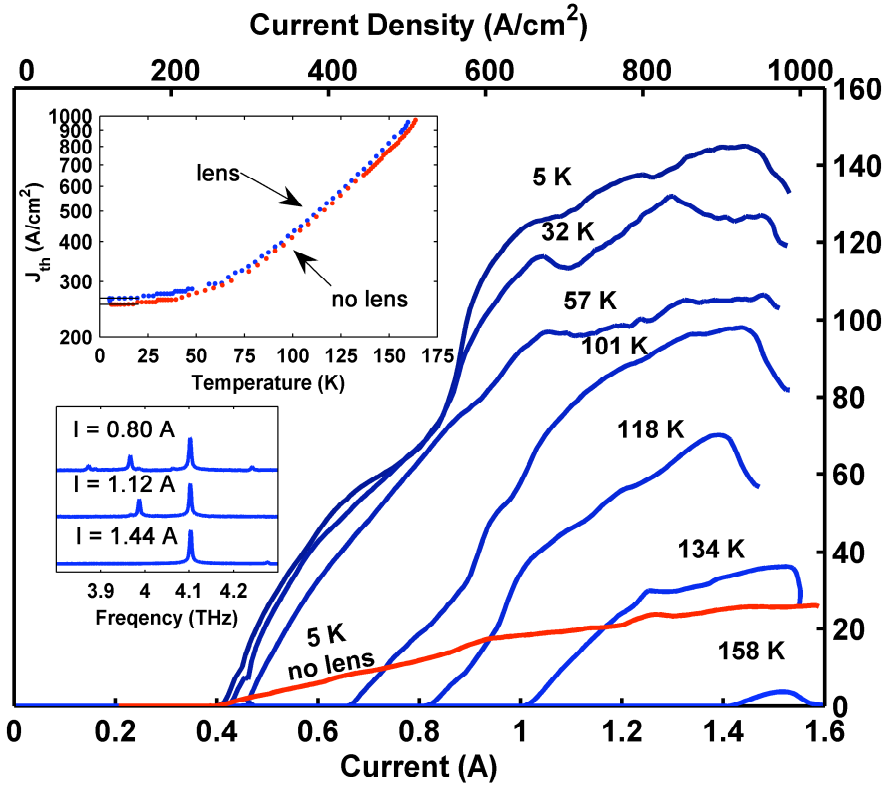


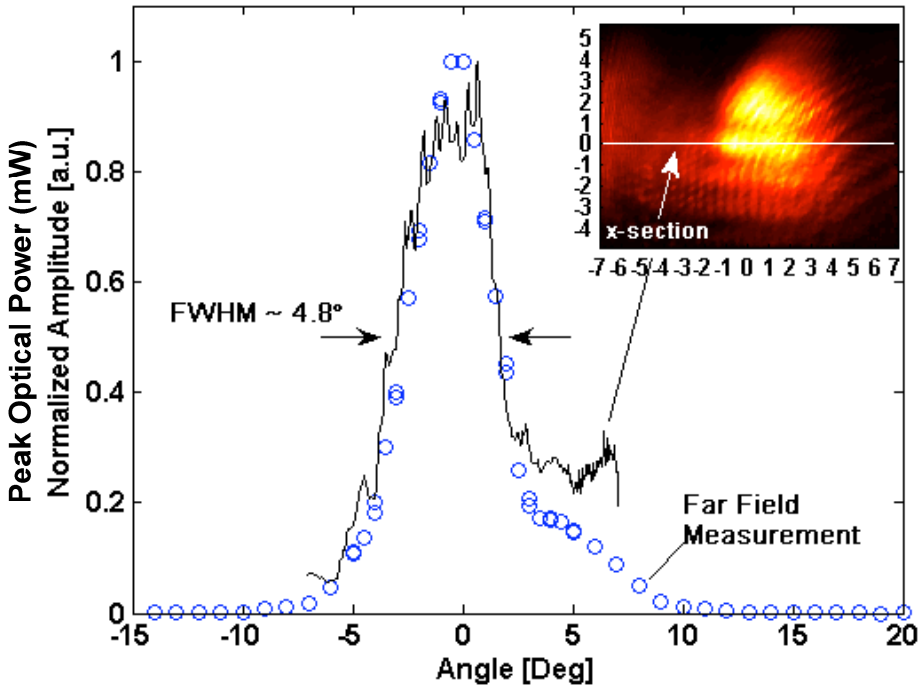


- $P_{MAX}$ = 145 mW and 26 mW without a lens (5.6x)
- $T_{MAX}$ = 160 K and 165 K without a lens
- wallplug power efficiency ~0.7%
- much tighter beam patterns

# Real-time THz imaging using QCLs and focal-plane array cameras

(A. W. M. Lee and Q. Hu, Opt. Lett. **30**, 2563 (2005),
A.W.M. Lee *et al.* PTL **18**, 1415 (2006))

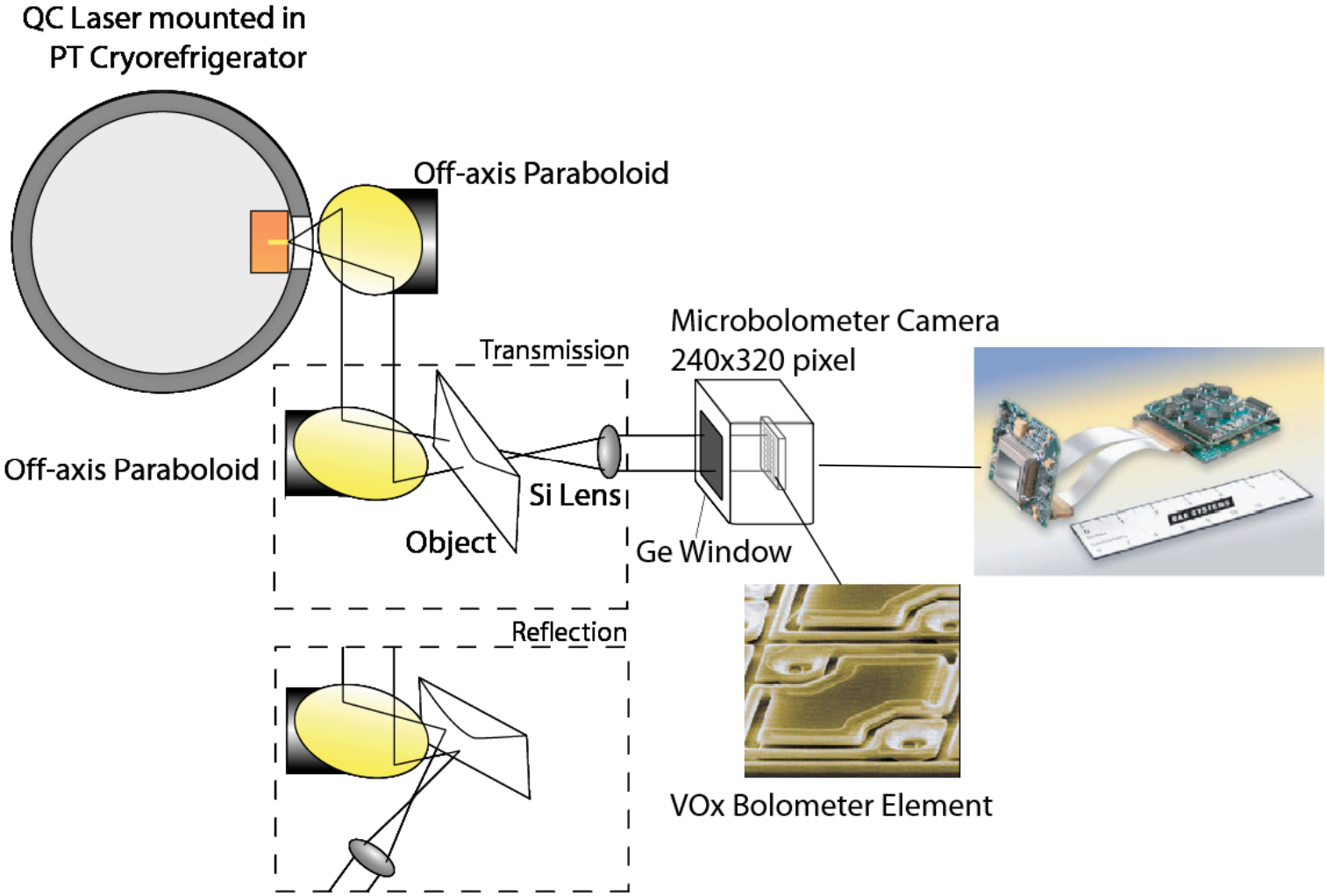

# Microbolometer-array cameras

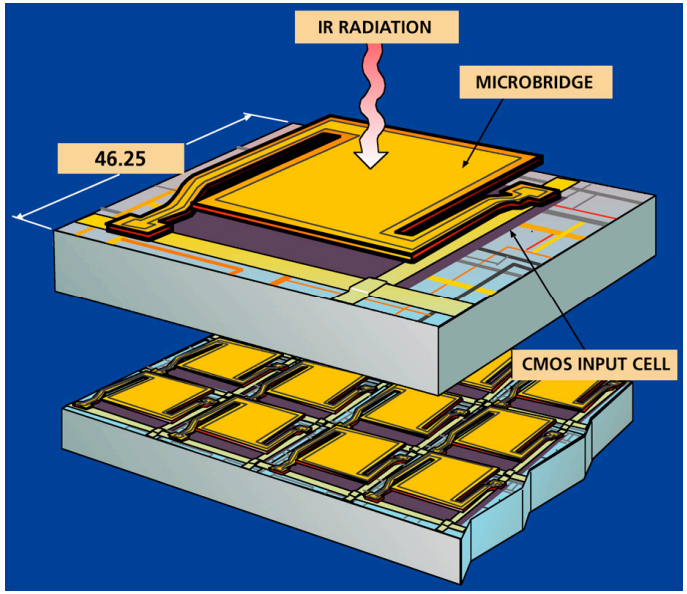


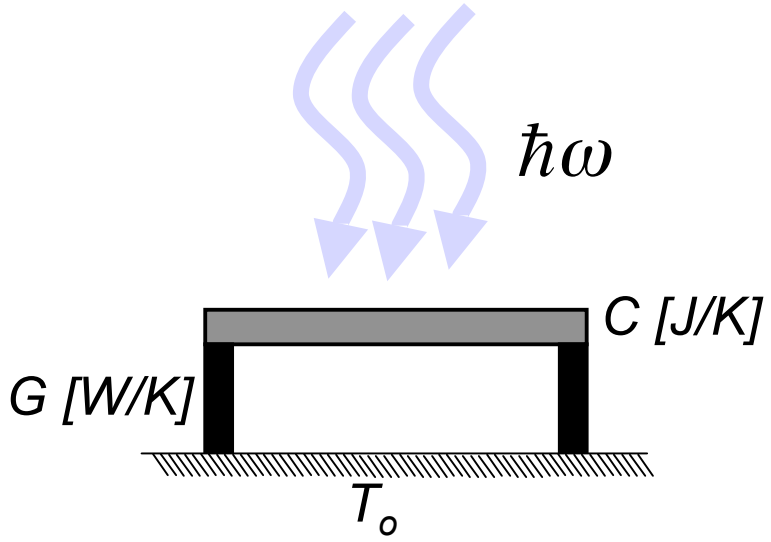


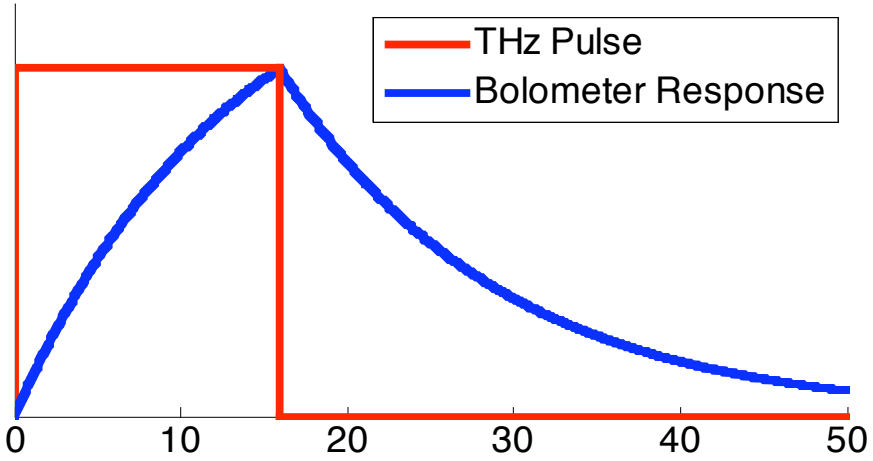


$$T_{bolo} = T_o + \frac{P}{G}\left(1 - e^{-\frac{t}{\tau}}\right), \quad \tau = \frac{C}{G} \approx 13 \text{ ms}$$

- $VO_x$ as thermometer
- video rate (60 frame/s)
- electrical NEP ~ 1 pW/√ Hz

# Differential Scheme for Real-time Imaging

*Frame Acquisition Sequence:*

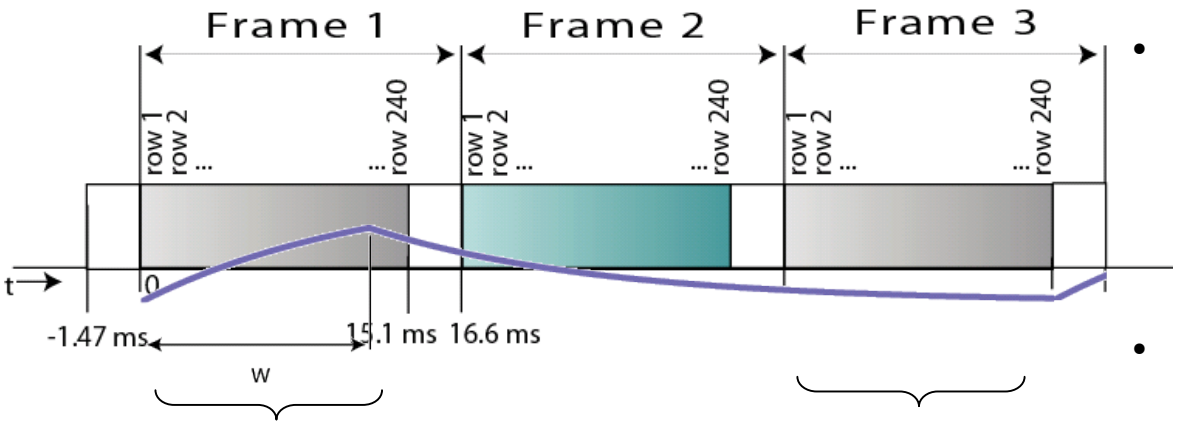


- Night vision cameras most sensitive to 7–14 $\mu$m wavelengths, overwhelms THz signals.
- Differential scheme removes strong infrared background and reduce 1/*f* noise.

**THz + Background**

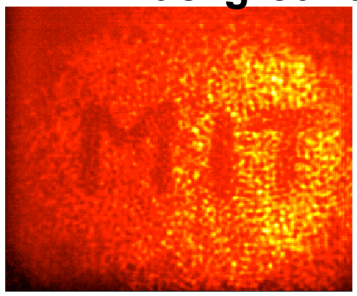

**Background**

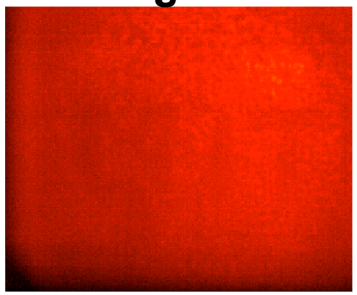

**THz**

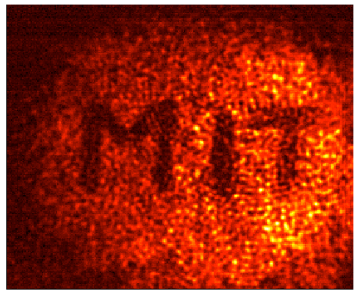

*Electronic Noise Spectrum:*

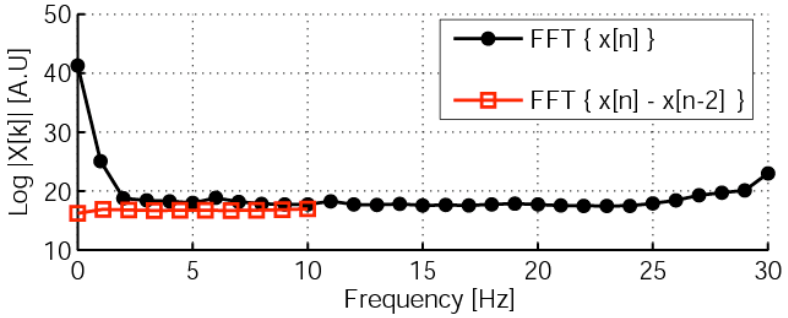

# Real-time THz Videos

## Plastic Mechanical Pencil

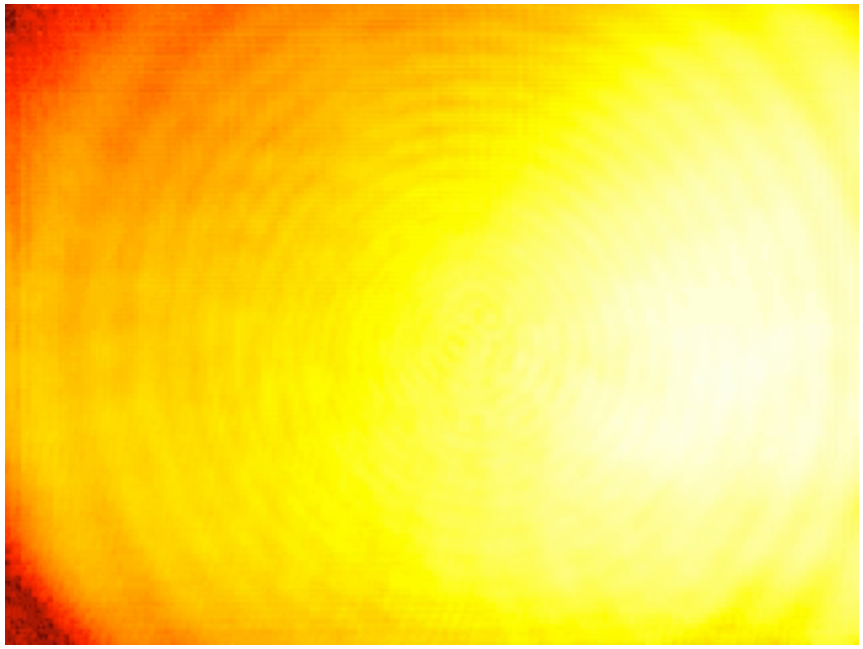

-4.3 THz (68 um)
-48 mW peak power
-Using f/1 -- 25 mm Si Lens
-320x240 pixel VOx microbolometer camera
-SNR ~ 200
-Images shown in log scale (light color represents high intensity)

# Real-time THz Videos

Metal Cutouts in Paper Envelope

# Real-time THz Videos

Dried Leaf

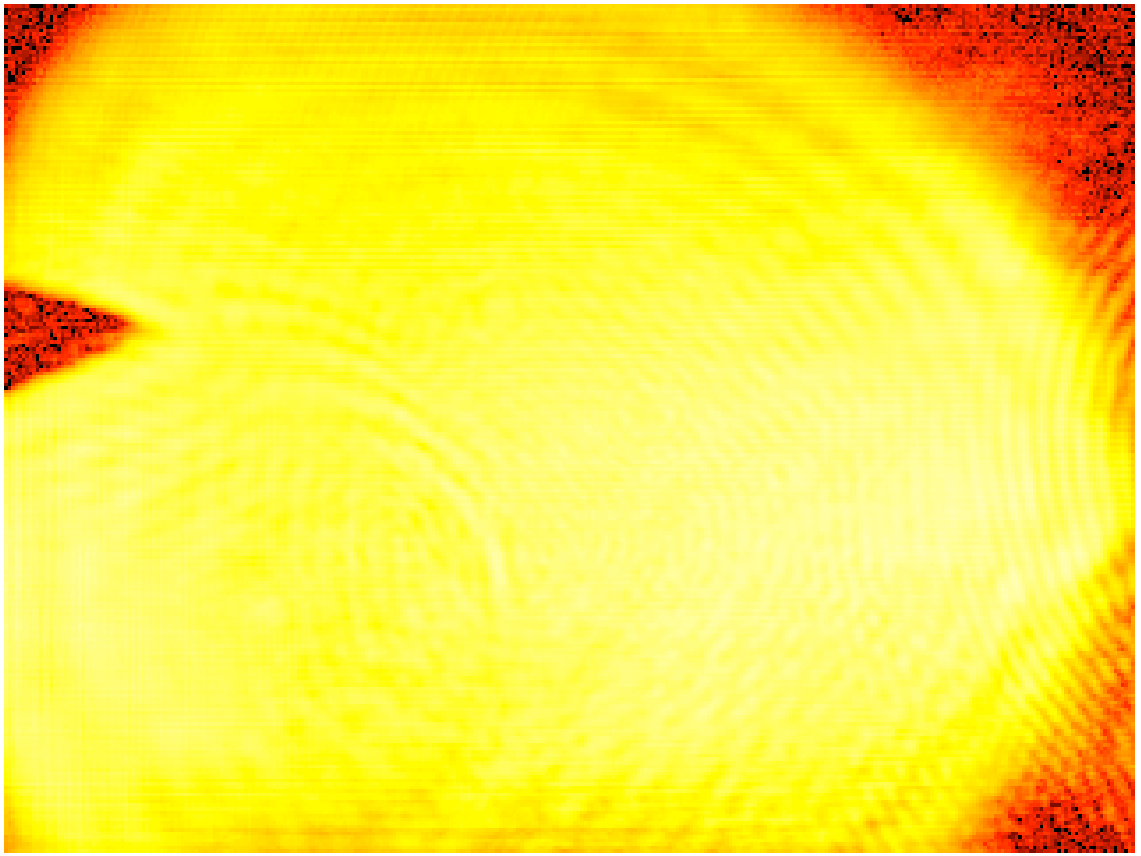

# Real-time THz Videos

Polystyrene block with an embedded metal screw

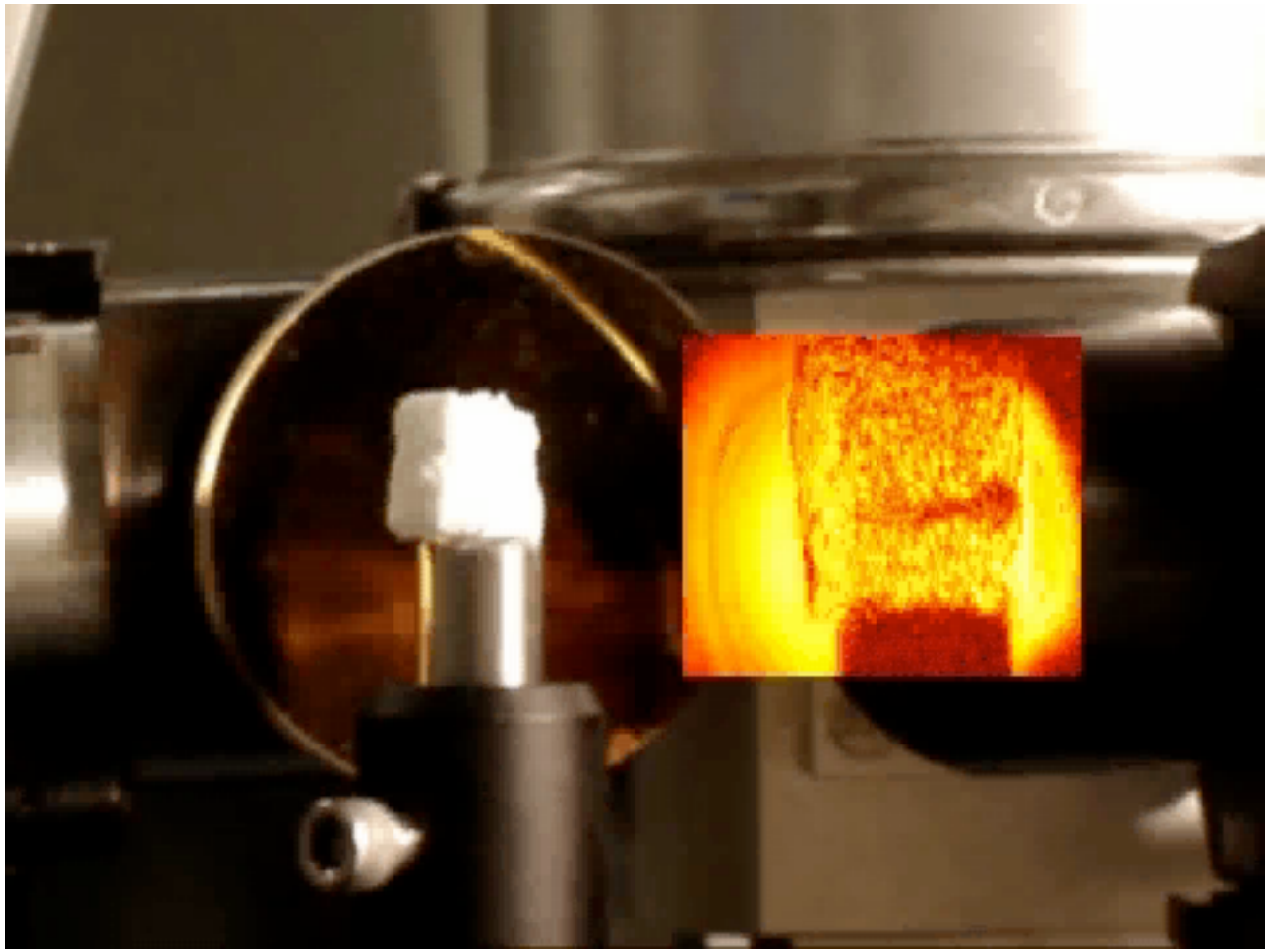

# Real-time THz Videos

Pencil hand writing inside a paper envelope

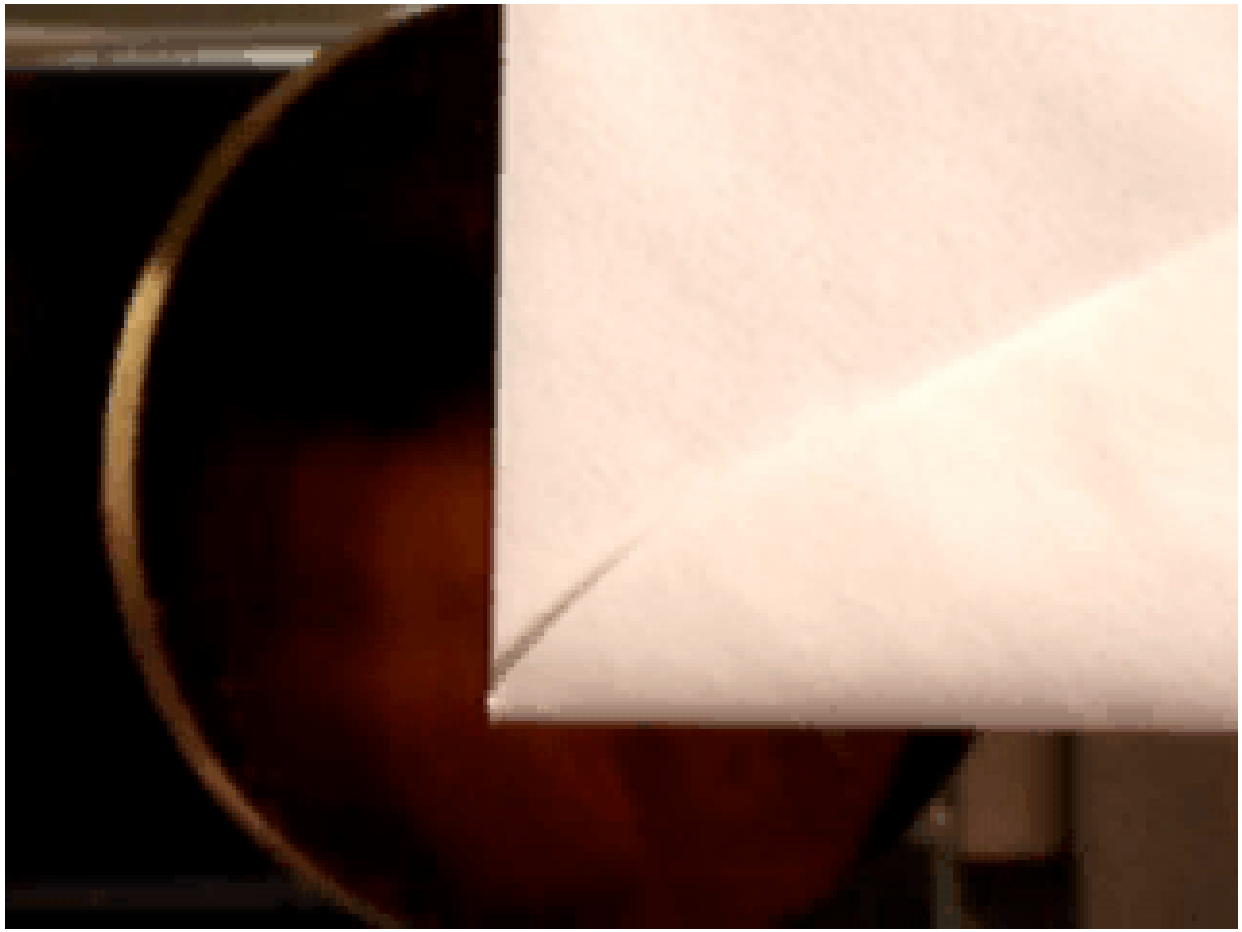

# Real-time THz imaging over long distance

**Most important issue:** It is frequency, frequency, and frequency!

Because of exponential attenuation in space, $P = P_o e^{-\alpha L}$, range only increases *logarithmically* with power.

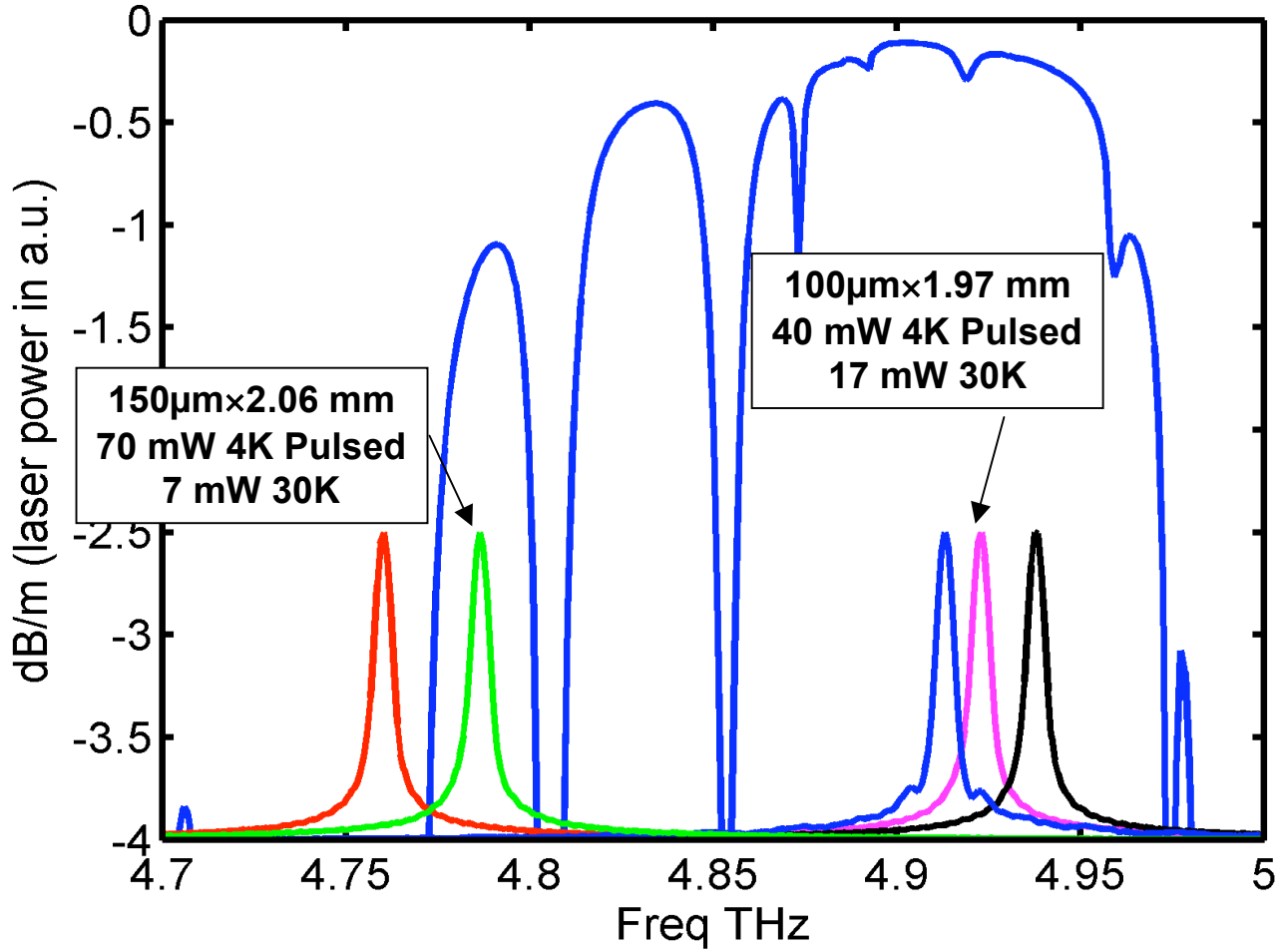

# Real-time THz imaging over stand-off range (>25 meters)

(Alan Lee *et al.* APL **89**, 141125 (2006))

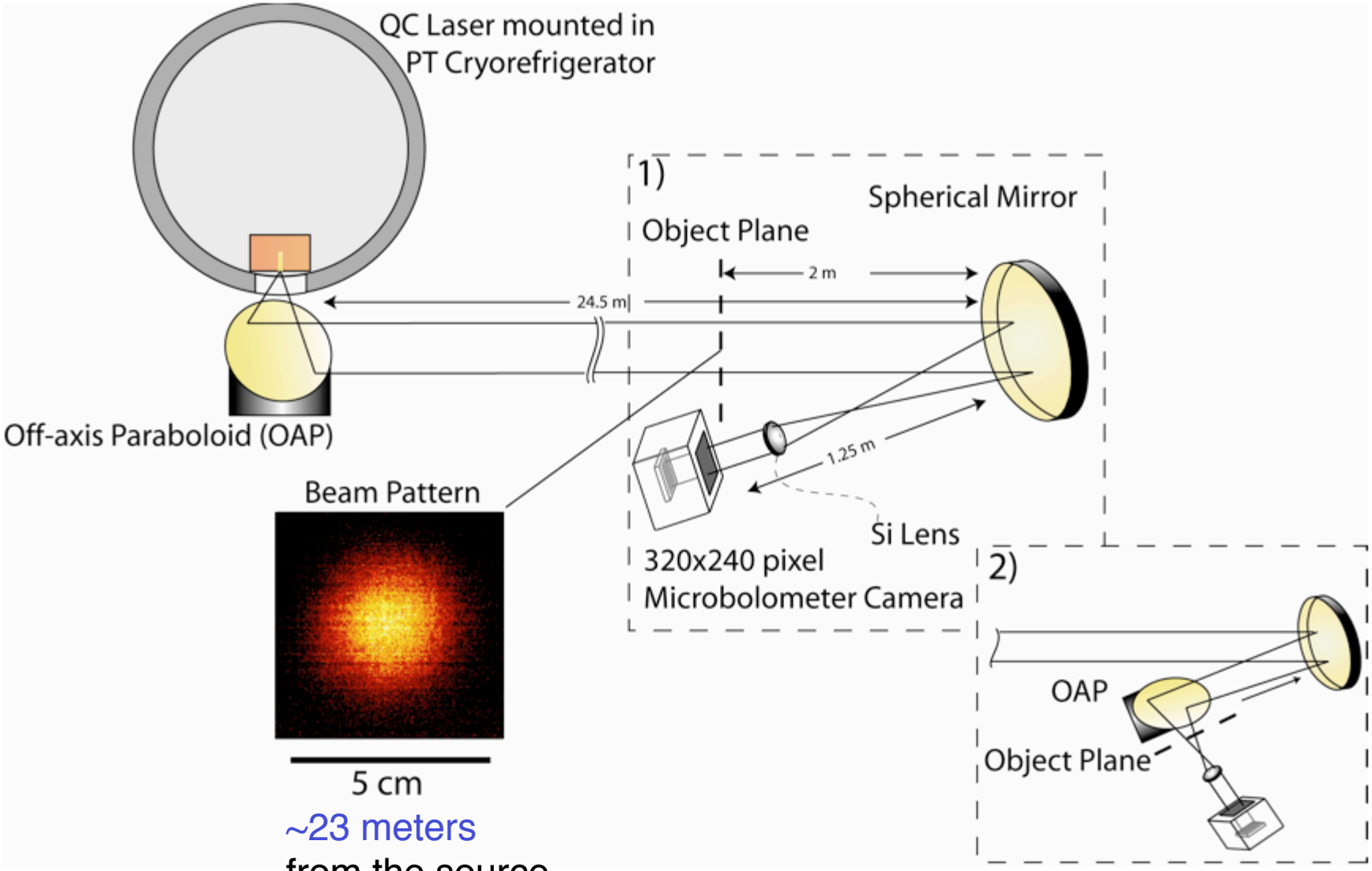


~23 meters
from the source

# Transmissive image over stand-off range (>25 meters)

(Alan Lee *et al.* APL **89**, 141125 (2006))

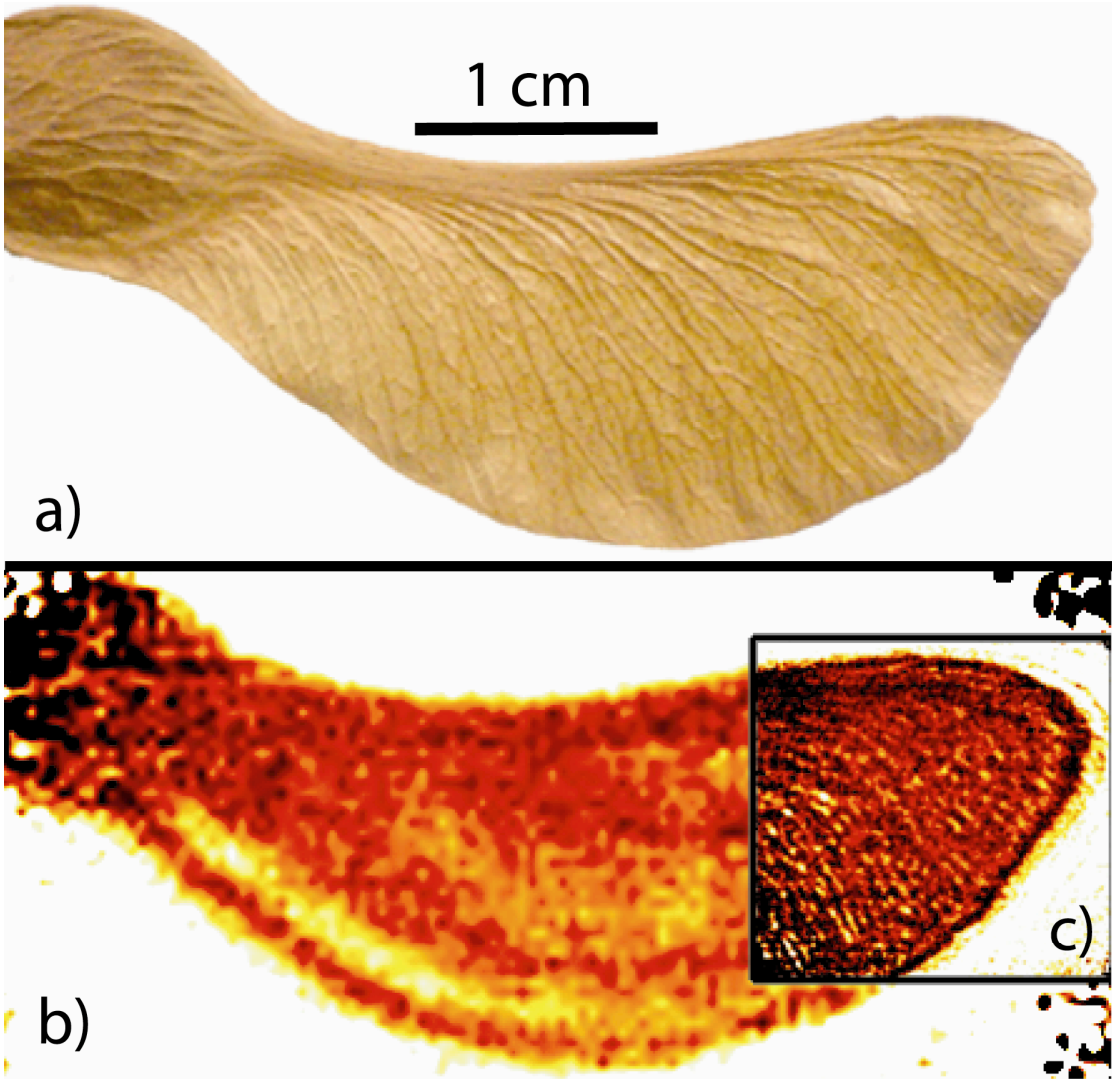

# Analysis of transport properties in THz QCLs

H. Callebaut et al.

- The key issue to improve THz QCLs' performance (especially the temperature performance) is the transport property. However, transport properties in THz QCL structures are complicated because of two special features at THz.

  — Scattering times are not constant, and they depend on electron density and temperature. Thus, the rate equations are nonlinear.

  — Dephasing (~4 meV) is important for tunnel injection through a barrier with $\Delta \sim 1$ meV.

# Monte Carlo Simulation

Use periodic BC, unique for QCLs, no fitting parameters. (R.Iotti and F. Rossi, APL, **78**, 2902, (2001))

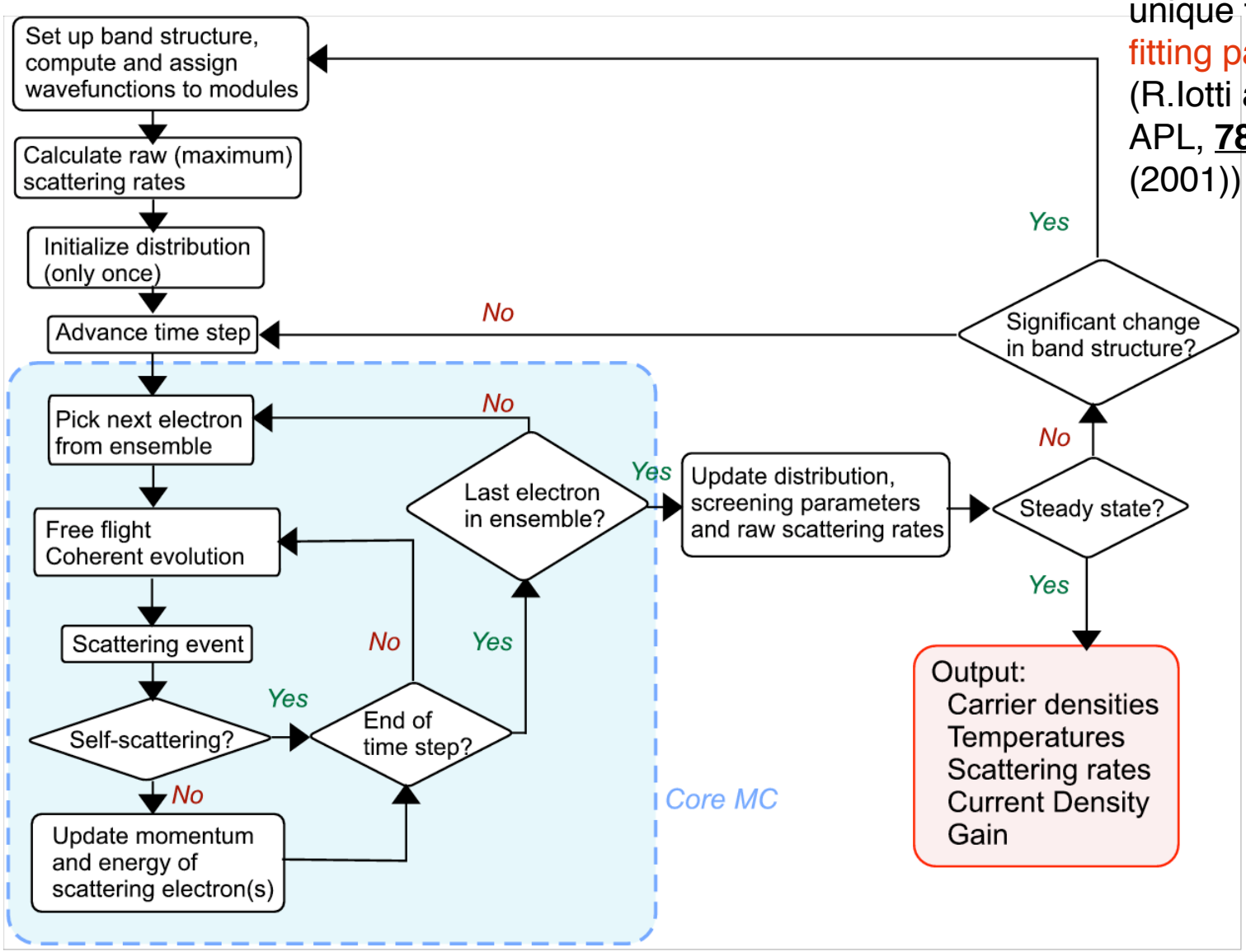

# Monte Carlo Simulation (cont.)

- Achieved only mixed results. For example, predicted gain in the simple three-level structure (with only two wells per module) but no lasing was achieved. Need to deal with *dephasing.*

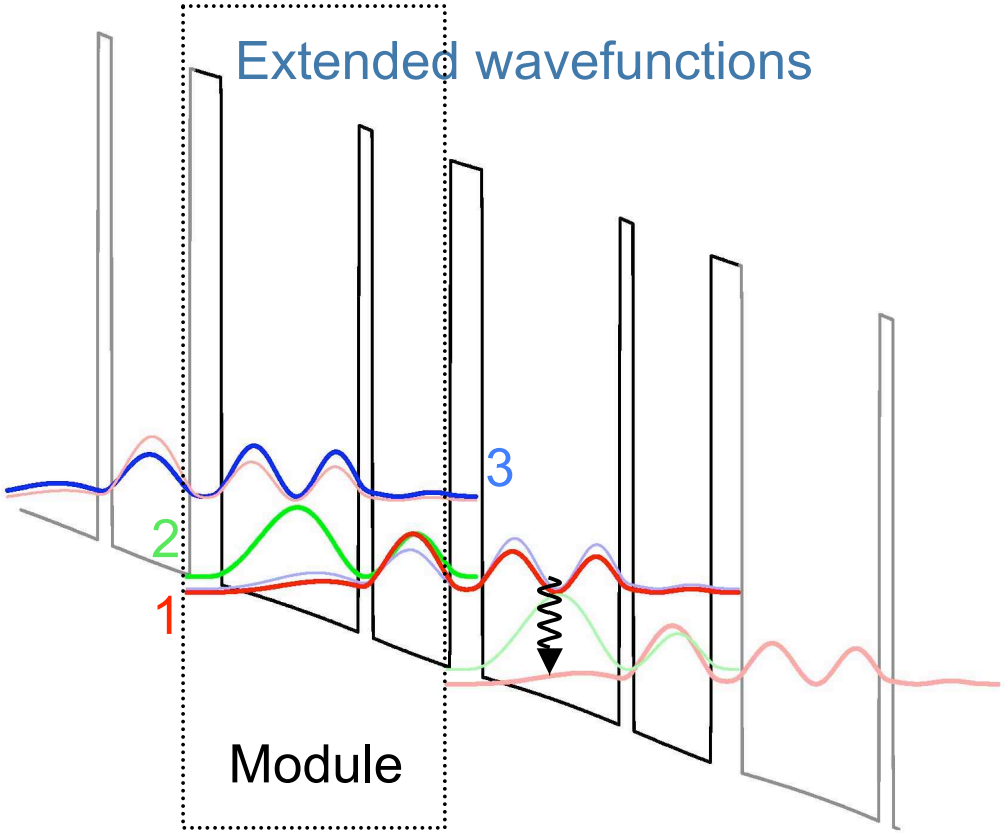


Semiclassical model

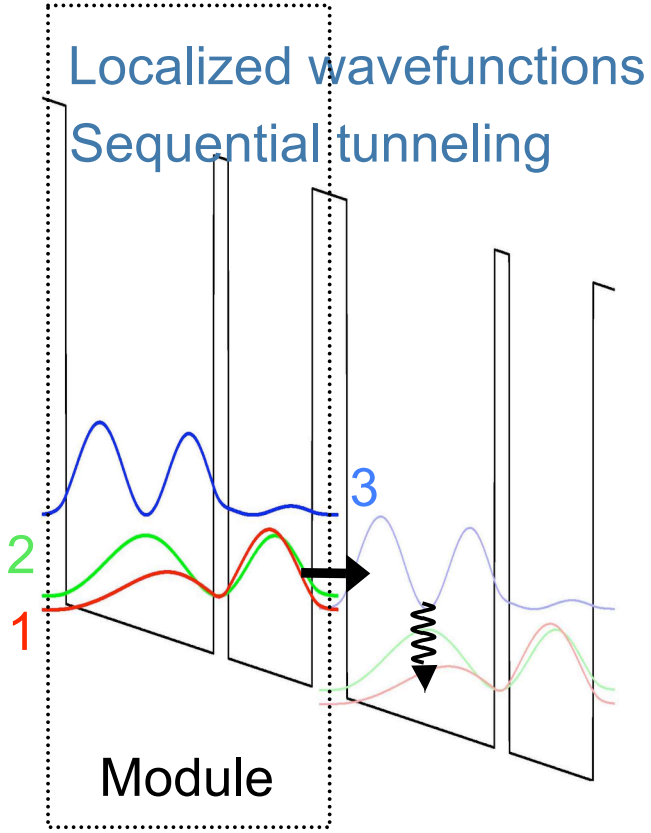


Tunneling model

# Semi-classical vs. Density Matrix & TBM

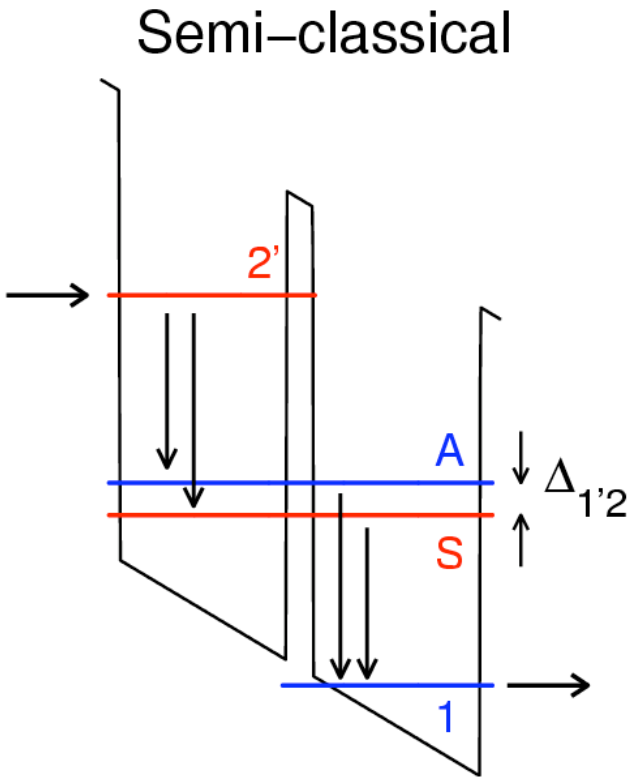


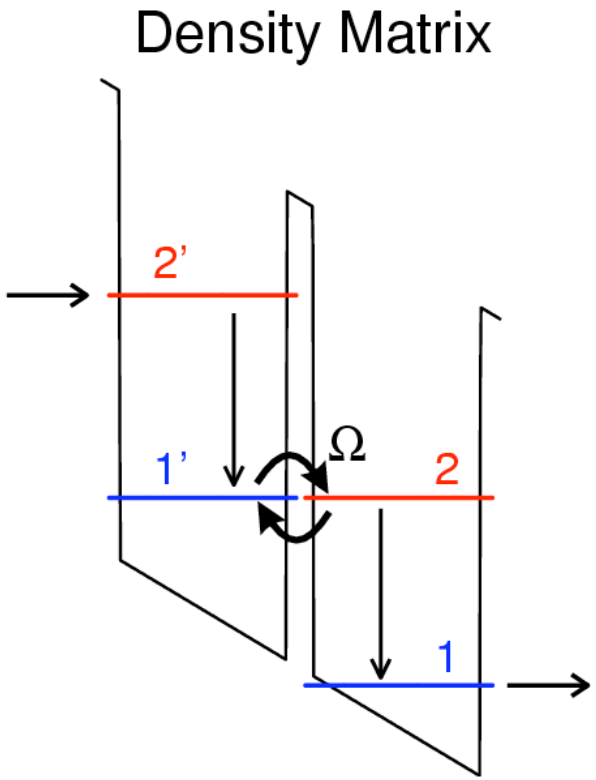


- No dephasing
- Delocalized levels A and S
- Barrier poses no resistance
- No phase information

- Localized levels 1' and 2
- Rabi oscillation $\omega = \Delta_{1'2}/h$
- Dephasing reduces J
- Keep track of phase information

# Dephasing

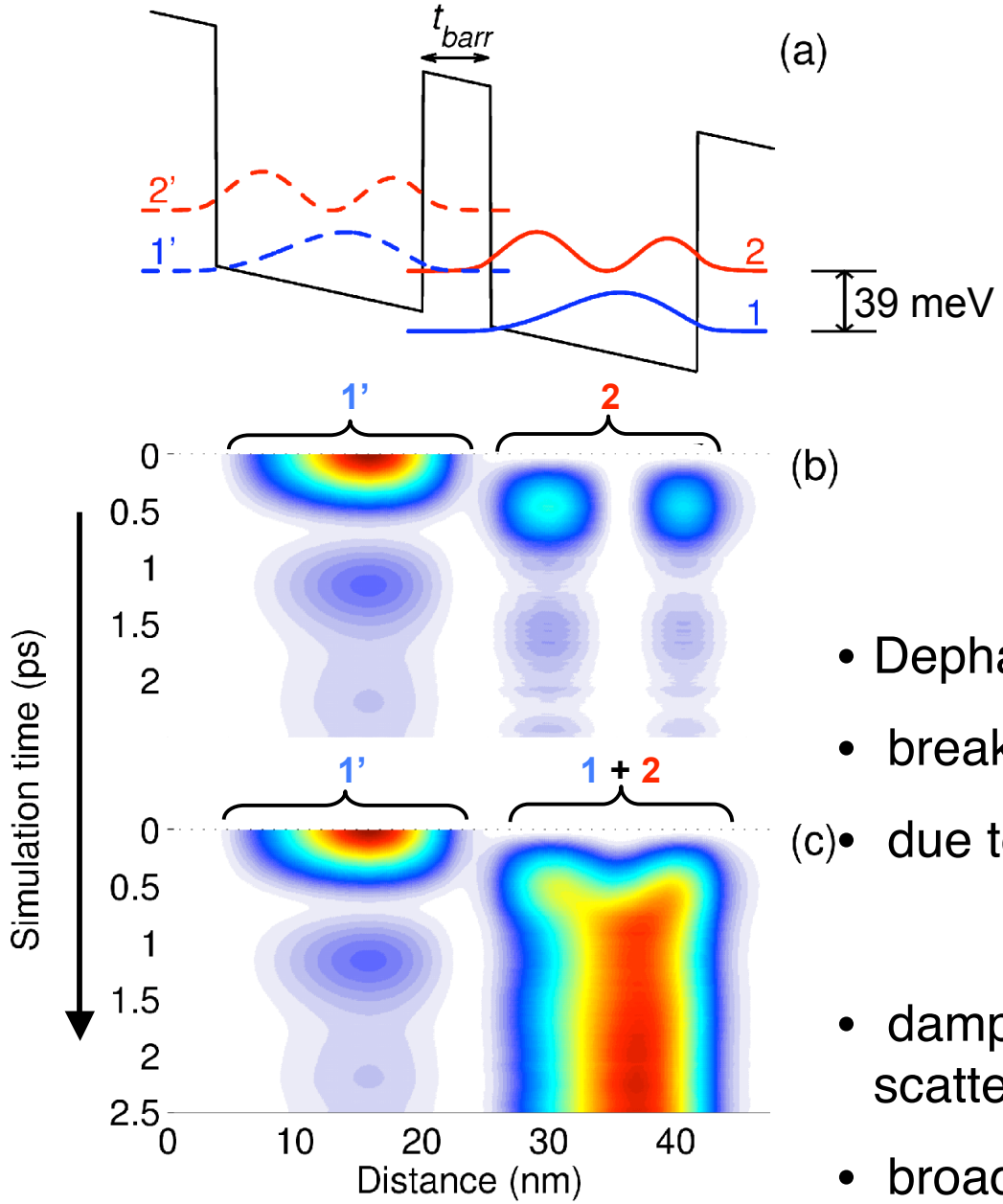


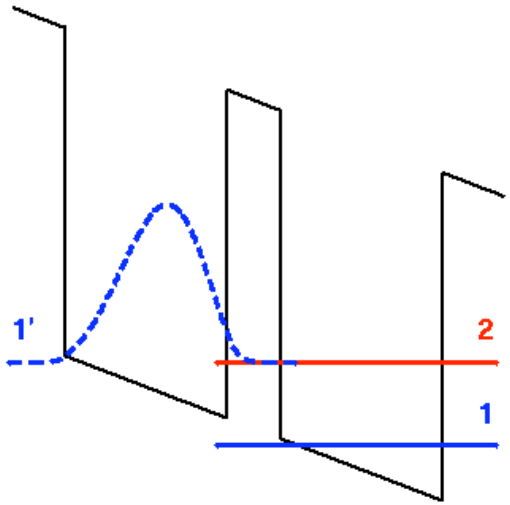


(c)

- Dephasing $T_{deph}$:
- breaks coherence of electron transport
- due to scattering $T_1$, pure dephasing $T_2$

$$T_{deph}^{-1}=(2T_1)^{-1}+T_2^{-1}$$

- dampens oscillation even if no scattering
- broadens energy level

# Effect of dephasing on transport

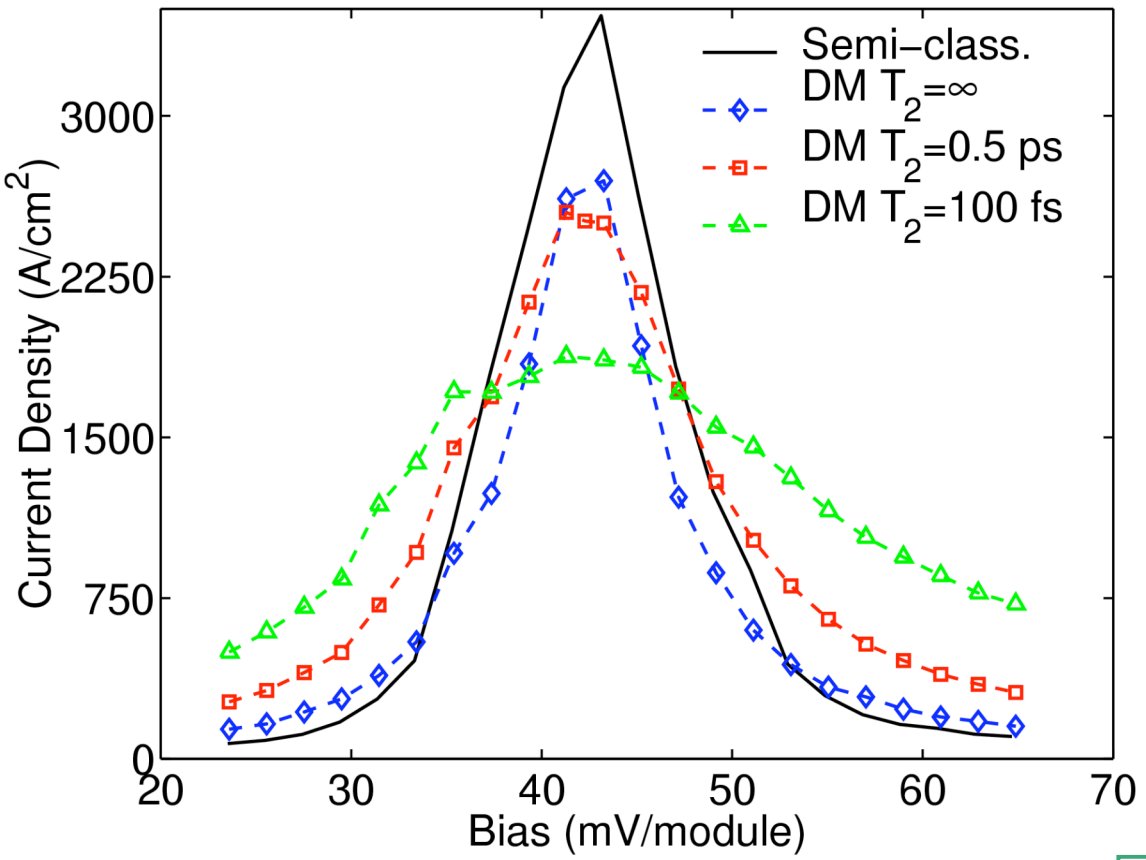


$\Delta_{1'2}$=4.5 meV

$E_{21}$=41 meV

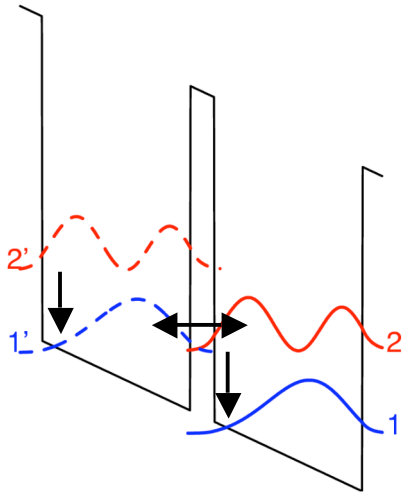


- Peak current density decreases
- Broadening of current peak (Lorentzian)
- Depopulation selectivity decreases

$$J = qN \frac{2|\Omega|^2 T_1}{1 + \Delta^2 T_1^2 + 4|\Omega|^2 T_1 T_2}$$

# Dephasing and anticrossing

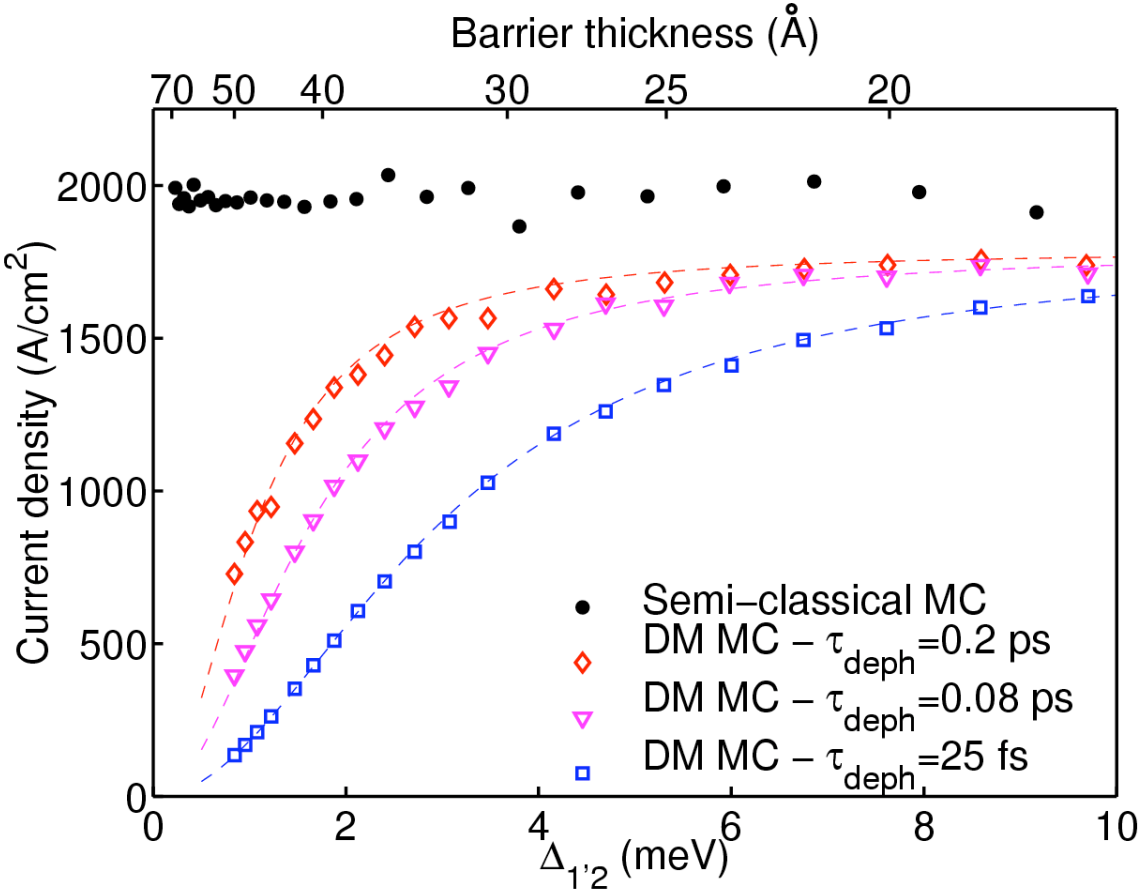


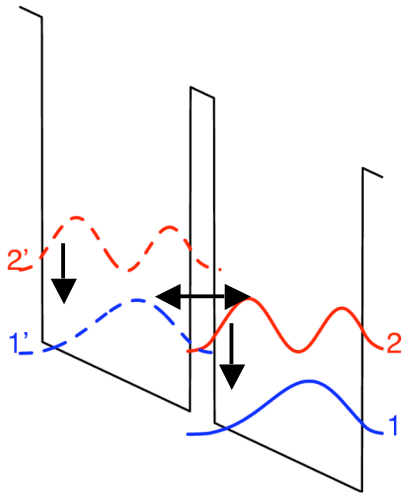


Density Matrix :

- Barrier thickness ↑ ⇒ $J_{peak}$ ↓
- $\tau_{deph}$=0.2 ps : roll-off $\Delta_{1'2}$ = 3 meV

Semi-classical:

Barrier thickness and $\Delta_{1'2}$ have no effect on $J_{peak} = \frac{qN_s}{2T_1}$

# Non-Equilibrium Green's (NEG) Functions

## Density Matrix :

- phenomenological dephasing
- "arbitrary" localization determines coherent transport

## Non-equilibrium Green's Functions:

- More generalized:
  - quantum-coherent effects
  - scattering to arbitrary order of perturbation
- Roots in many-body theory:
  - electrons interacting with electrons, ions, phonons
  - quasi-particles
  - self-energy
- Disadvantages:
  - Not very intuitive and complex
  - Computationally intensive: simplified version with momentum independent scattering

# NEGF Flowchart

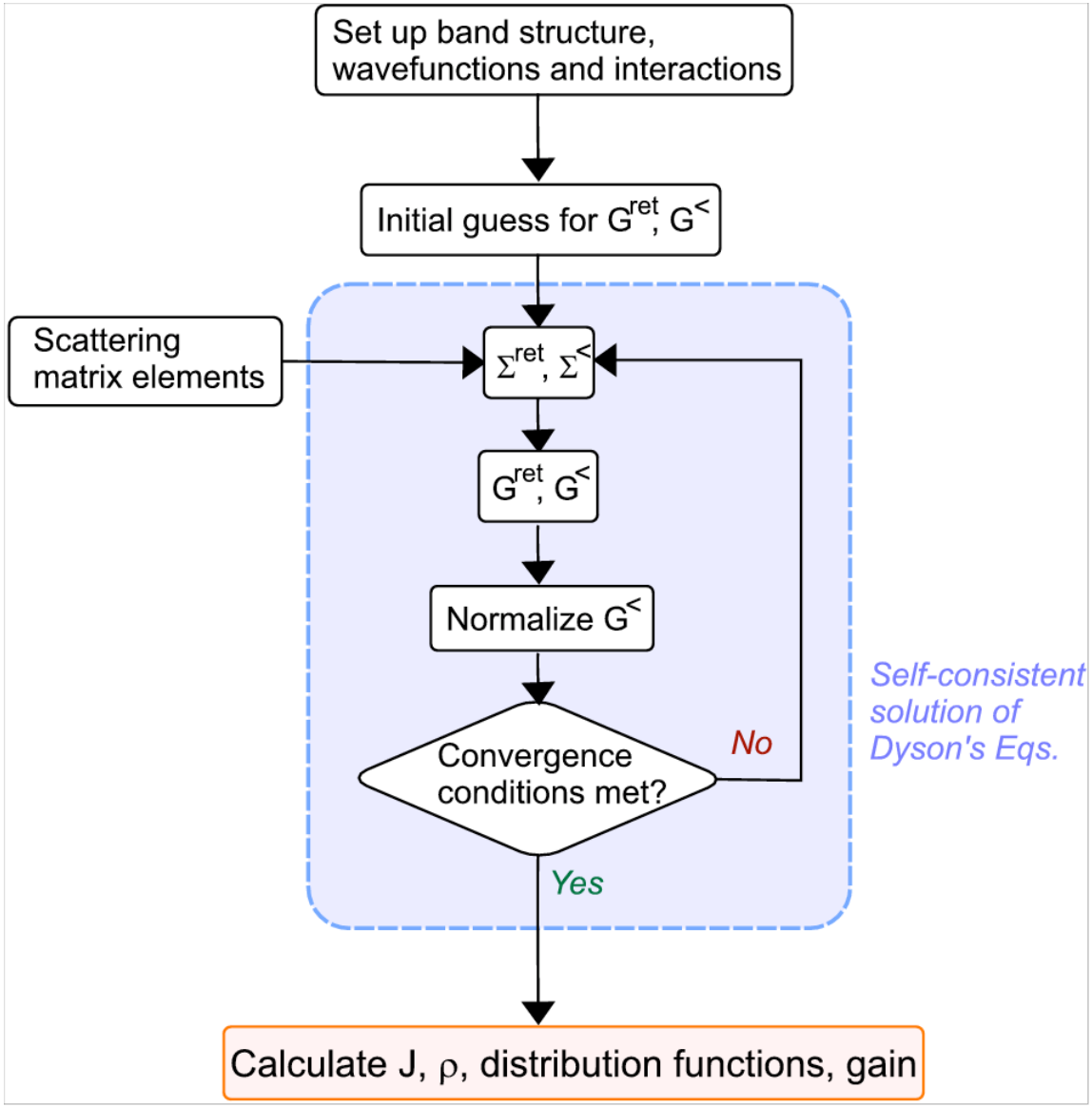

# T65: 3-level structure revisited

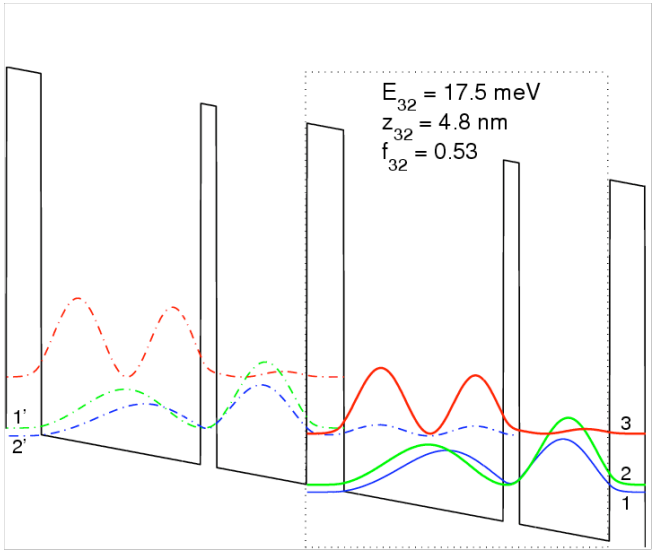


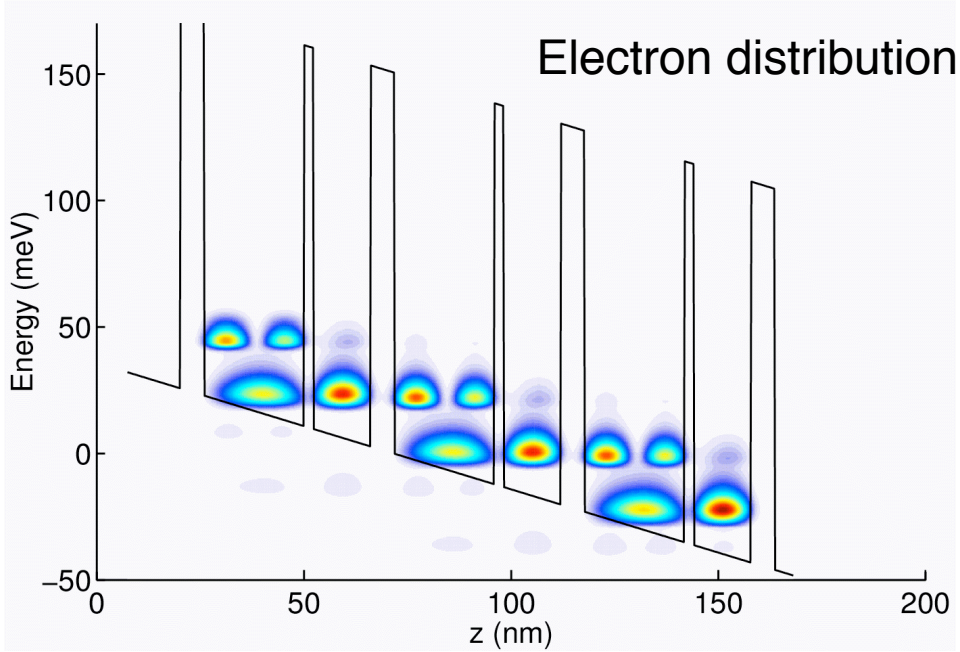


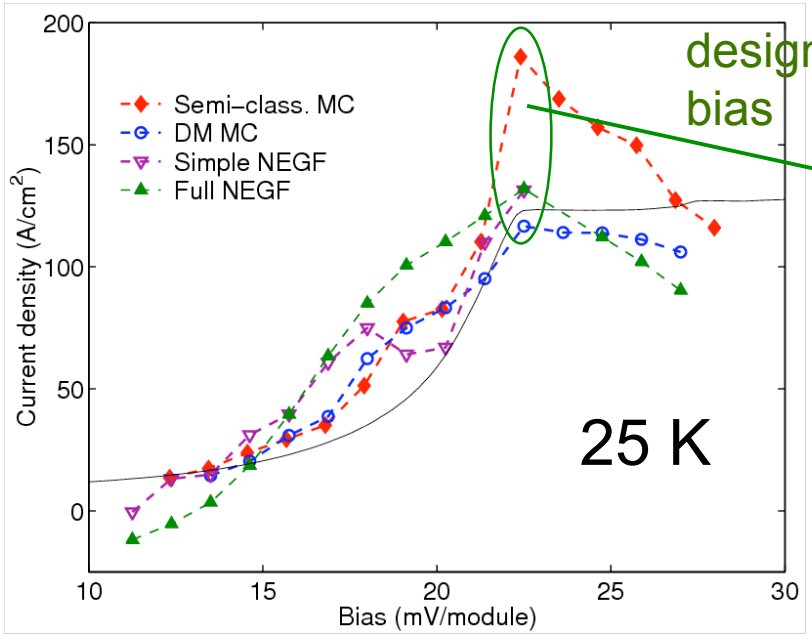


design bias

| subband | *Pop. ($10^9$ cm$^{-2}$)* | | |
|---|---|---|---|
| | Semicl. | DM-MC | NEG |
| 1 | 9.6 | 8.5 | 6.9 |
| 2 | 3.2 | 5.4 | 6.8 |
| 3 | 5.2 | 4.1 | 4.6 |

No gain!

# Required development for future applications

- For near-term applications (sensing)
  - >1 mW CW power at 80 K,
  - within ~2-4 GHz from the target line,
  - good beam patterns,
  - frequency/phase locked to the harmonic of a low-frequency reference,
  - power dissipation < 2 W.

- For long-term applications
  - Increase the operating temperatures, initially to TE cooler temperature, ultimately above room-temperature operation.
  - Develop THz QCLs with better beam patterns and higher power levels.
  - Develop THz QCLs over a broad frequency range of 1-7 THz.
  - Develop broadly frequency tunable THz QCLs for local oscillator, imaging, and spectroscopy applications.
  - Develop THz amplifiers based on the QCL structures

# Scattering mechanisms in THz QCL structures

Population inversion:

$$\Delta N = \frac{J}{e}\tau_3\left(1-\frac{\tau_2}{\tau_{32}}\right)$$

must have $\tau_{32} > \tau_2$

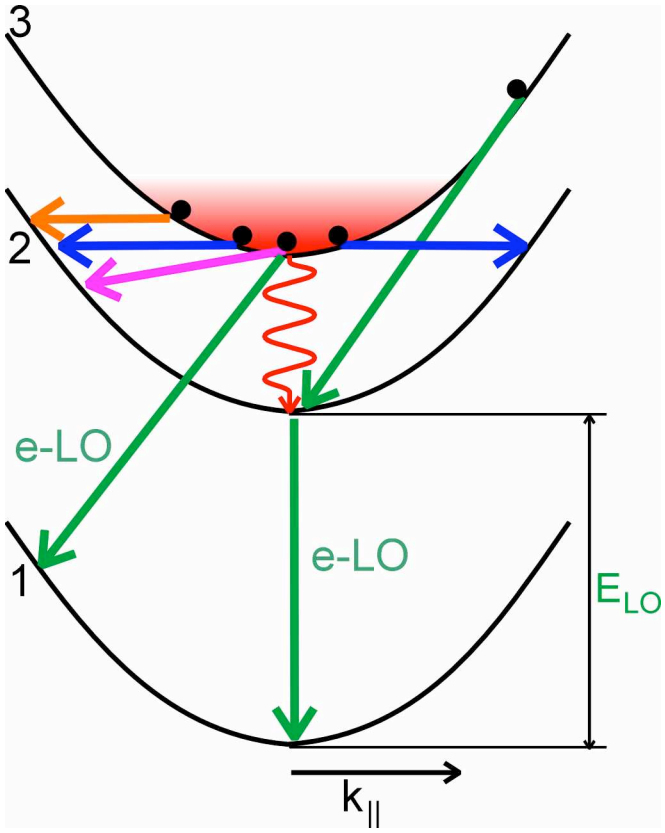


$\tau_{21} < 1$ ps depopulation (e-LO)

$\tau_{32,rad} \sim 10\,\mu s$ radiative lifetime

$\tau_{e-LA} \sim 100$ ps acoustic-phonon

$\tau_{e-imp} \sim 7 - 20$ ps impurity scattering

$\tau_{e-\mathrm{int}} \sim 10$ ps ??? interface roughness

$\tau_{e-e} \sim 5 - 50$ ps ? electron-electron

thermally activated e-LO

$$\tau^{-1}_{e-LO,hot} \approx \tau^{-1}_{LO}\exp\left(\frac{\hbar\omega - E_{LO}}{k_B T_e}\right)$$